Aircraft Performance Parameter Estimation using Global ADS-B and Open Data

Thijs W. Gloudemans*

TU Delft, Delft, Zuid Holland, 2629HS, Netherlands

To enable low cost open source ATM simulations the University of Technology Delft is developing an open source ATM simulator Bluesky. A method was developed to identify aircraft performance parameters using ADS-B and other open sources of data. The goal is to determine the operational flight envelope and get estimates for the lift- and drag coefficients. The method streams global ADS-B data from Flightradar24. By making assumptions on wind and flight strategies, estimation can be obtained for aircraft parameters. The nature of these assumptions limit the aircraft types being analyzed to commercial aircraft only. The method measures the operational flight envelope and estimates weight, lift and drag coefficients for multiple phases in flight. Next the operational flight envelope was compared to open data. Here it was found that the estimations showed similar values as the open data and that the operational flight envelope can be estimated using the method. The drag polar was compared to BADA, which showed a consistent underestimation of the drag polar.

Nomenclature

V_∞	True air speed
α_∞	Acceleration, m/s^2
s	Distance, m
M	Mach number
W	Weight, N
T	Thrust, N
L	Lift, N
D	Drag, N
C_L	Lift coefficient
C_D	Drag coefficient
$C_{D,0}$	Zero-lift drag coefficient
K	Induced drag coefficient
γ	Flight path angle
ϕ	Bank angle
ψ	Heading angle
ρ	Air density
S	Aircraft wing surface
ψ	Heading angle

I. Introduction

With the introduction of Bluesky[1] in 2013, the Air Traffic Management (ATM) department of the Delft University of Technology (DUT) is developing a free and open source real- and fast-time air traffic simulator. The goal of Bluesky is to provide everybody who wants to visualize, analyze or simulate air traffic with a

*Graduate student, Faculty of Aerospace Engineering, Kluyverweg 1 tool to do so without any restrictions, licenses or limitations. The current version of Bluesky can be used for ATM and Air Traffic Flow (ATF) simulations. Bluesky provides the user with a graphical user interface showing selected traffic flows in real- or fast-time on a map. The user can load traffic scenarios, influence aircraft's behaviors and perform metric analysis.

At the core of Bluesky are two aircraft performance models (APMs). The first APM is the Base of Aircraft Data (BADA). BADA is a proprietary APM developed by Eurocontrol. Since the proprietary characteristic conflicts with the goal to develop an open source and free ATM simulator, also a Bluesky APM is under development. One of the major difficulties in developing an APM lies with the identification of these proprietary aircraft type-specific parameters, such as the operational flight envelope or the lift and drag coefficients. For some aircraft these parameters can be found in literature, but the parameters for most modern commercial airliners are not published by their manufacturers. The aircraft type-specific parameters are key parameters for proper aircraft modeling. Many different aircraft types exist, all of them having different modeling parameters. Identifying these parameters is therefore important when making an APM.

The basis of this research lies in the new ability to use the wealth of data that automatic dependent surveillance - broadcast (ADS-B) messages provide. Global networks of ADS-B receivers allow for continuous surveillance of the global airspace. The assumption is that this new source of Big Data can reveal knowledge of aircraft flight performance that was previously only available to manufacturers, operators and air traffic control. The goal of this research is to find or estimate the operational flight envelope. Also efforts are made to estimate the lift- and drag coefficients. This knowledge can then be used to improve the Bluesky APM. It must be noted that this is an ambitious goal, with some large hurdles in the way such as aircraft weight estimation. The priority in this research is to obtain results and to set out the steps necessary to get them. This might lead to the use of simplified methods and assumptions. The major requirement for the use of methods and assumptions is that they can be enhanced in future research.

ADS-B is a secondary surveillance system. An aircraft equipped with an ADS-B transponder will continuously broadcast flight information such as position, speed, altitude and heading. The data used in the analysis is obtained from Flightradar24.[2] Flightradar24 is an application that bundles ADS-B data obtained from many ADS-B receivers around the world and projects the data on a map. This allows users to track flights in almost real-time. With a premium account it is possible to query the Application Program Interface (API) for the state of the global airspace. The terms of usage of this account allow for unlimited processing and redistribution of these data, making Flightradar24 an ideal source for large amounts of historical flight data.

To unravel the knowledge from the ADS-B data a structured approach is used. The process can be described by six subsequent steps, namely; understanding the problem, understanding the data, preparation of the data, data mining, evaluation and implementation. Some of these steps are iterative. This article is setup according to these steps. Although the first two steps have been performed in preliminary research a short recap will be provided for completeness. Next the method, which composes the preparation and the data mining steps, is discussed. Finally the results are discussed and an evaluation is performed.

I.A. Background

The need for APMs has been of significant importance to many stakeholders in industry for a long time. In 1971, Boeing and NASA worked together on an APM for the B747.[3] This six degree of freedom APM was not only needed for use in ATM concepts, but also for use in flight training simulators and control design. These dynamic models were capable of predicting dynamic and kinematic behavior relatively well. In their tests NASA and Boeing determined the aerodynamic and control coefficients from in-flight measurements. This made the model expensive to obtain.

Researchers came up with other, cheaper methods, that suited ATM research better. In the 70s the EROCOA and the PARZOC[4] were developed. The EROCOA method is a technique which describes the climb performance of aircraft by using a set of 8 coefficients. In a similar fashion identical performance for the en-route and descent could be obtained from the PARZOC approach. Using these methods the vertical profile of aircraft flying defined speed regimes could be computed through parametric models. Although initially designed for use in flight profile prediction modules for application in on-line ATC systems, these approaches proved also suitable for use as aircraft models in ATM simulators.

With the increase in computational power, many different ATM simulators were developed, such as ASTOR,[5] ACES,[6] TMX[7] and many more. Most of them started off with an in-house developed APM. In the early 1990s EUROCONTROL started developing BADA,[8] an APM database. The initial goal of BADA was to realistically simulate en-route aircraft behavior under nominal operating conditions, while ensuring large coverage of aircraft types.

BADA APM is based on a kinetic approach to aircraft performance modeling. It is made of two components. The first component are the model specifications. The model specifications provide the theoretical fundamentals used to calculate aircraft performance parameters. The second component are the datasets. The datasets contain the aircraft-specific coefficients necessary to perform calculations. Nowadays most ATM simulators use the BADA APM. For example the ACES simulator can use both the Kinematic Trajectory Generator (KTG)[9] as the Multi Purpose Aircraft Simulation (MPAS).[6] Both are used to model aircraft performance, but at the base of these simulators or generators is the BADA performance database.

The BADA database is built using radar data from EUROCONTROL. Even though BADA is widely accepted as the standard it is not flawless. BADA uses reference data to validate its models.[10] This reference data is generally obtained from Aircraft Operation Manuals (AOMs), but some manufacturers provide performance data. The drawback of these AOMs is that the resolution of the data provided can be very low and only applies to general situations.[11] This could lead to errors in the model.

Where BADA uses the radar data, everybody else can use ADS-B. As part of international cooperation ADS-B has been cast as the next generation aircraft surveillance method and will be mandatory for aviation in many parts of the world by 2020.[12] The broadcast characteristic of ADS-B makes it suitable for large scale monitoring. Everyone with an ADS-B receiver can track flights. With a global network of ADS-B receivers it would be possible to track all flights in the air. Aircraft equipped with ADS-B broadcast altitude, ground speed, latitude, longitude, heading, ICAO identification and call sign.

Using this data, one of the major pillars of BADA has become available to the public, namely the track data. The other source of data used in BADA such as the AOMs remain closed source, but open alternatives exist. Most manufacturers place key parameters such as weights, dimensions, engine types and capacity on their website.[13] Other parameters such as fuel flow can be obtained from the ICAO Engine Emissions Databank.[14] Combining all these open sources a non proprietary APM could be constructed by performing a similar system identification as BADA does. This research strives to be the initiator by identifying the operation flight envelope and estimations for lift- and drag coefficients for the most used aircraft types.

A crucial component in this analysis is wind. Aircraft performance is very dependent on true air speed, but ADS-B only provides ground speed. To determine the true air speed using the ground speed the wind speed and direction need to be known. Since this research is an initial attempt to use ADS-B for aircraft system identification the wind is not taken into account. Within the scope of this research this assumption is justified for simplicity. Extending this method with weather estimations would be possible, since a lot of research has been performed in meteorological modeling.

The major issue with meteorological modeling is the high degree of non-linearity and dependency on initial conditions. This is called the 'butterfly effect'.[15] For systems that show the 'butterfly effect', small changes in the initial condition can have large influence on the output. The atmosphere shows this effect and obtaining good, distributed measurements is difficult. These errors in the measurements propagate through the system, potentially creating very different output. Therefore it is only possible to have good predictions for only a few hours. Many weather stations perform atmospheric soundings every 12 hours to gather input data for the models. Much of this sounding data is open and can be downloaded.[16]

Two large organizations provide global weather forecasts using frequent observations. The first is the European Centre for Medium-Range Weather Forecasts (ECMWF). ECMWF is an international organization that provides weather forecasts to the national weather centers of the European Union. The model that they use is the Integrated Forecast System (IFS), which is a proprietary model. The second center is the National Center for Environmental Prediction (NCEP). The model used by NCEP is the Global Forecast System (GFS). These two models are extensively used for aviation forecasts and can provide reasonable wind predictions. Unlike IFS the GFS output is free and open and can thus be used in subsequent versions of this analysis.

So far ADS-B has not been extensively used for aircraft parameter identification, but some applications have been discussed in literature. These are discussed next.

I.B. Previous Research

Networks of ADS-B receivers started to emerge around 2006 and large global networks were not available until 2009. Researchers could only use partial tracks obtained from their receivers, which have a limited range. In 2009 Delahaye[17,18] tried to estimate the true air speed from ADS-B. The methods developed looked at turning aircraft and subsequently at the change in speed during the turn. To extract a wind measurement from a radar track of a turning aircraft, the vehicle's velocity in the y-direction was plotted against its x-direction velocity. If there was no wind, the aircraft would maintain a constant speed with respect to both the air and the ground. Using the wind vector and the ground speed it is then possible to determine the true air speed.

Recently Sun[19] proposed two methods to determine the aircraft mass based on ADS-B data. Sun states that given standard atmospheric and wind conditions the acceleration profile for an aircraft type is closely correlated with its weight. The two methods make use of this by looking at the intermediate measurements during take-off and the lift-off speed. This method is used as the basis for the weight estimation performed in this study. But instead of using lift-off speed the take-off distance is chosen.

To identify the phase of an aircraft, Sun[20] used fuzzy logic to classify a measurement as either ground, climb, cruise or descent. Based on the altitude, speed and rate of climb a measurement is assigned to one of the phases. Again this method will be used as basis for the current study. However there are some changes. The first change is the number of phases. This will be extended with 7 other phases to isolate phases with a specific lift configuration, such as take-off, initial climb and final approach. Sun does not provide a membership function for every phase, instead higher abstraction levels are used. For example an altitude can be low, medium or large. Although this leaves fewer membership functions it does make the inference more challenging, because it requires the levels to be assigned to the phases. Another disadvantage is that it makes tuning of the membership functions more difficult, because changing a membership function will influences multiple phases.

Due to the small time that ADS-B is available it has not extensively been used for performance parameter estimation. It mainly has been used to determine wind speed and direction. The KNMI tried to perform upper airspace measurements using ADS-B data.[21] For these measurements they not only decoded the ADS-B message, but also other Mode S messages that were received. Decoding these messages gives access to interesting parameters such as pressure altitude and indicated air speed. A large difference here is that those messages are not available on a global level, because the aircraft transponder needs to be interrogated by ATC for it to respond with the Mode S message.

In 2012 de Leege[22] extended two methods to estimate wind using ADS-B data. The first method is based on Delahaye,[17,18] which was discussed above. The second method is based on the assumption that aircraft at the same altitude travel, on average, at the same true air speed in all directions. This enables estimating wind for a larger area at fixed time and altitude intervals.[23]

Aircraft performance has been researched the last few years, but not by the use of ADS-B. In 2014 Alligier[24] used machine learning algorithms to estimate the mass and thrust of an aircraft in climb. The data used was obtained from the Paris Air Traffic Control center, which included flight trajectories, Mode C and weather reports. The data from ATC, as with the Mode S, contains more information than ADS-B making this method not compatible with the goal of this research.

I.C. Understanding the Data

Quickly stated, the goal is to find the operational flight envelope and lift- and drag coefficients using ADS-B data and other open sources. The first step is to reflect upon which data is available. First there is the ADS-B data, which consist of altitude h, ground speed V_{gr}, heading ψ, latitude, longitude, call sign and ICAO number. On top of the ADS-B data, Flightradar24 also provides the aircraft model, destination, origin, rate of climb V_{roc} and a time stamp for each flight measurement. This data is updated approximately every 5 seconds for each aircraft that has its ADS-B transponder turned on and is within Flightradar24 coverage. Such a set of ADS-B data will be called a measurement from now on.

For each aircraft type the following weights are known; maximum take of weight W_{MTOW}, maximum landing weight W_{MLW}, zero fuel weight, W_{ZFW}, operating empty weight W_{OEW} and maximum fuel weight W_{MFW}.[25,26] The aircraft dimensions are known, but only the wing surface area S is used. For every aircraft type the most used aircraft engine types are known.[14] The corresponding fuel mass flows for take-off $\dot{m}_{to}$, cruise $\dot{m}_{cr}$, approach $\dot{m}_{ap}$ and idle $\dot{m}_{idle}$ are available. Also the rated thrust T_{max} at sea level is known. Finally the thrust specific fuel consumption c_t is also found.[27]

Using this the operational flight envelope can be determined. The operational flight envelope is defined here as the operational limits, which are minimum true air speed $V_{TAS_{min}}$, maximum true air speed $V_{TAS_{max}}$, maximum altitude h_{max}, minimum rate of climb $V_{roc_{min}}$, maximum rate of climb $V_{roc_{max}}$, minimum turn radius R_{min}. Load limits are not taken into account, because it can be safely assumed no flying aircraft will come close to its limits.

II. Method

II.A. Operational Flight Envelope

Now that there is an understanding of the available data the first parameters can be determined. The first parameter to be determined is the true air speed V_{TAS} because it is a required parameter in many mathematical relations. As discussed earlier no wind estimations are known. Therefore the V_{TAS} is assumed to be the sum of the velocity vectors V_{gr} and V_{roc} as seen in Equation 1.

$$V_{TAS} = \sqrt{V_{gr}^2 + V_{roc}^2} \tag{1}$$

The next parameter to be calculated is the flight path angle γ. Again this can be determined using V_{gr} and V_{roc} given in Equation 2.

$$\gamma = arctan(\frac{V_{roc}}{V_{gr}}) \tag{2}$$

Now using each subsequent measurement in the measurement signal the discrete time derivatives, $\dot{V}_{TAS}$, $\dot{V}_{roc}$, $\dot{\psi}$ and $\dot{\gamma}$ can be determined.

The parameters calculated so far combined with the measurement is what will be referred to as the state of the aircraft. The operational flight envelope can be determined from all the determined states of an aircraft type. This allows finding the minima and maxima of the whole flight, but this leaves the question in which phase this minimum or maximum occurs. During a flight an aircraft will go through multiple flight phases. Each phase has its own flight strategy and operation. Knowing the minima and maxima for all these flight phases is more interesting than just for the whole flight. Therefore each flight is classified into different phases.

The method used is an extended version of Suns[20] method. The major difference is that the number of phases is increased to make a distinction between phases where the aircraft is in high-lift configuration. The flights are separated into 12 phases, namely; ground, take-off, landing, initial climb, climb, cruise climb, cruise, horizontal flight, initial descent, descent, final approach and miscellaneous. In each of these phases the type of flight differs from another. For example the difference between initial climb and climb is the configuration an aircraft is in. In initial climb the aircraft is generally in a high-lift configuration to be able to lift-off, while in climb the flaps are retracted to clean configuration. Another example is cruise and the horizontal flight. The main difference is altitude, but the major goal is to separate aircraft that are in climb or descent but need to maintain altitude due to ATC from actual cruising aircraft.

The classification is done using fuzzy logic. All the phases except ground, landing and take-off are classified based on V_{TAS}, h and V_{roc}. The only distinction between ground, landing and take-off is acceleration $\dot{V}_{TAS}$. Therefore these phases are also classified based on $\dot{V}_{TAS}$. Taking the derivative of a noisy signal will increase the noise. It is difficult to use $\dot{V}_{TAS}$ for classification directly. A choice is made to smoothen $\dot{V}_{TAS}$ before classification. This is done using a moving average with a window of 4 measurements.

In Figure 1 the membership functions of the fuzzy logic are shown. Every phase has its own membership function per variable. Inference is performed by finding the phase with the maximum degree of membership. Membership degree is determined by multiplying each membership degree for each variable as shown in Equation 3.

$$f_{phase} = ms_{V_{phase}} ms_{h_{phase}} ms_{roc_{phase}} \tag{3}$$

Here f_{phase} is the degree of membership for a phase. $ms_{V_{phase}}$, $ms_{h_{phase}}$ and $ms_{roc_{phase}}$ are respectively the degrees of membership for the variables V_{TAS}, h and V_{roc}. For the ground phases ground, take-off and landing also the membership degree of $\dot{V}_{TAS}$ is added. Next the measurement is assigned to the phase with the highest degree of membership.

$$Phase = argmax([f_{ground}, f_{takeoff}, ..., f_{finalapproach}, f_{landing}]) \tag{4}$$

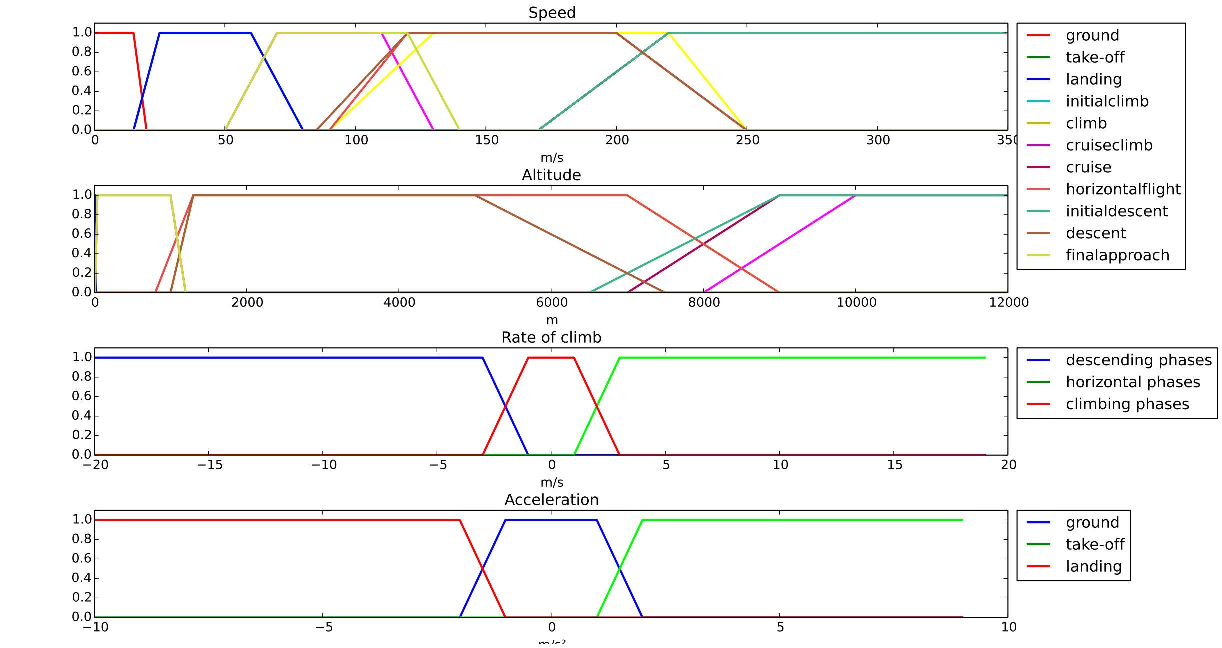

Figure 1. Membership functions used for classification

When all membership degrees are zero the measurement is classified as noise. In Figure 2 the resulting classification of a B737-800 flight can be seen.

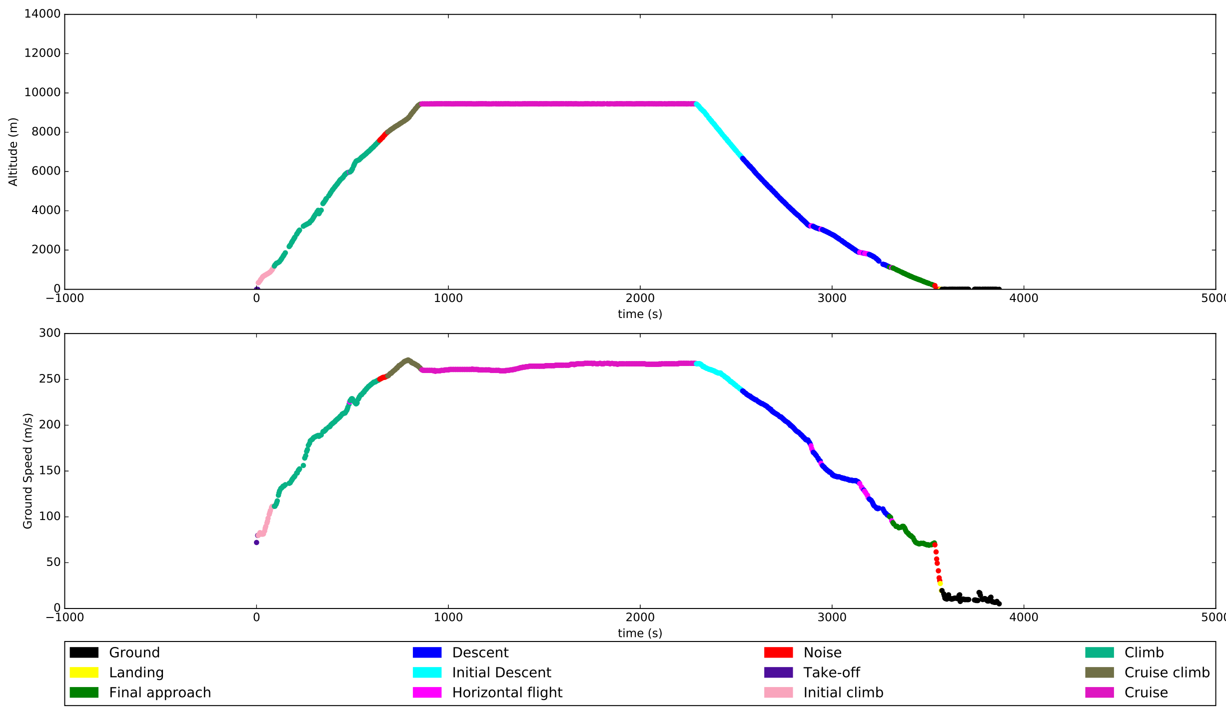

Figure 2. Flight B737-800 different phases

The quality of this method depends on the quality of the tuning. The membership functions are manually generated and differ for each aircraft type. Proper configuration requires some background knowledge of the aircraft. Errors in configuration could cause a measurement to be assigned noise when it could have been assigned to a phase. The percentage of noise for classifying phases for a B737-800 are around 1.5%. This includes falsely identified noise. This percentage for the Airbus A320 currently is 2.6%.

Now that each aircraft state is classified it becomes possible to start performing statistical analysis. With each measurement and corresponding full state the parameters in the state are binned, the mean is calculated and standard deviation is updated. When a value is larger than the current maximum this value is set as the maximum with the limitation that it cannot be larger than three times the standard deviation. This limit is introduced to make sure that the minimum or maximum will not be set by noise. Next the lift- and drag coefficients are discussed.

II.B. Lift and Drag Coefficients

So far the method describes only how to obtain statistics from measurements and direct derivatives. But one of the goals of this research is to obtain an estimation for the lift- and drag coefficients C_L and C_D. Two major components for determining C_L and C_D are the aircraft weight W and the thrust T. These are not known and therefore need to be estimated first.

II.B.1. Aircraft Weight Estimation

Aircraft weight estimation in itself is already a very difficult topic for which many methods exist. They require a lot of assumptions and only work in a specific flight phase. Here a simple method is used for weight estimation. It is possible to try and estimate W during any moment of the flight, but this requires C_L, which is not available. The approach used here, similar to Sun,[19] is to determine the take-off weight. The weight is estimated based on the assumption that aircraft on average use similar thrust and flap settings for take-off. This leads to a longer take-off distance when the aircraft is heavier. It is also recognized that distance of flight influences the fuel weight needed for the flight. The method used divides the weight into three parts; empty, fuel and payload weight. The empty weight is known. The other two are calculated as follows.

$$W_{fuel} = \dot{m}_{cr} g_0 \frac{s_{total}}{V_{average}} \tag{5}$$

Where $\dot{m}_{cr}$[14] is the fuel mass flow in kg/s, s_{total} the flight distance and V_{mean} is the mean speed during cruise determined from all measured flights. The payload weight is determined by comparing the measured take-off distance s_{to} to the maximum of previous measured take-off distances.

$$W_{payload} = \frac{s_{TO}}{s_{TO_{max}}} W_{mplw} \tag{6}$$

Here $s_{TO_{max}}$ is the maximum take-off distance measured and W_{MPLW} is the maximum payload weight. Finally the total take-off weight is determined by summing up the three parts.

$$W_{TO} = W_{eow} + W_{fuel} + W_{payload} \tag{7}$$

By choosing to make only $W_{payload}$ dependent on measurements reduces the influence of noise.

II.B.2. Lift coefficient

Now that W has been estimated it is possible to estimate C_L. Assuming that the aircraft is in steady flight and $L = Wcos(\gamma)$ holds then C_L can be calculated using Equation 8.

$$C_L = \frac{2Wcos(\gamma)}{\rho V_{TAS}^2 S} \tag{8}$$

Earlier the point was made that splitting up the flight in multiple phases was advantageous to determine the flight envelope. Another reason to split up the flight in phases is the difference in C_L. The C_L is dependent on the aircraft configuration and angle of attack α. These are settings that are not known exactly, but high, medium and clean configurations can be expected. During take-off and initial climb the aircraft is in a medium high configuration after which it changes to clean configuration with a higher α. Until the descent phase the aircraft is in clean configuration. During final approach and landing the aircraft is in high configuration. By dividing the flight in phases an estimate for C_L can be gained for the different configurations. This is similar for C_D which is discussed next.

II.B.3. Drag coefficient

The last parameter to be found is the drag coefficient C_D. Determining C_D directly would require knowledge of T. Thrust settings are not known during analysis therefore other methods were explored which are limited to only climbing, cruise and descending phases.

During climb C_D can be estimated by assuming that $\frac{dT}{dV_{TAS}} = 0$. Although this is not true for the total climb it can be assumed true for just one time step. By using the excess power relation from Anderson[28] the change in D becomes equal to the change in excess thrust $(T - D)$. The excess thrust can be calculated from the Total Energy Equation obtained from Anderson.[28] Assuming that C_D is quasi constant it can be calculated as follows.

$$C_D = \frac{-1}{\rho_\infty V_{TAS} S} \frac{d(T-D)}{dV_{TAS}} \tag{9}$$

During cruise phase the excess force $(T - D)$ becomes zero, which makes the previous method unfit. On the other hand this condition does allow for another advantage, namely $T = D$. Using the thrust specific fuel consumption c_t and the change in weight ΔW the T can calculated. Except ΔW is not known. This is solved in the following manner.

For the cruise phase the C_L is determined for the first ten minutes of cruise. For the remainder of the cruise C_L is assumed to be constant and equal to the just determined C_L. Assuming that $L_n = W_n$ the discrete time derivative of the weight can be calculated using Equation 10.

$$\frac{\Delta W}{\Delta t} = \frac{L_n - W_{n-1}}{\Delta t} = \frac{0.5 C_{L_n} \rho_{\infty_n} V_{TAS_n}^2 S - W_{n-1}}{\Delta t} \tag{10}$$

Here n is the n-th measurement. This change in W is only caused by fuel burn. The T can be derived by dividing the change in weight with the thrust specific fuel consumption. This is shown in Equation 11.

$$T = -\frac{\Delta W}{\Delta t} \frac{1}{c_T} \tag{11}$$

During cruise it is assumed that $T = D$. Subsequently T can substitute D in the drag equation from Anderson.[28] This leads to Equation 12.

$$C_D = \frac{2T}{\rho_\infty V_{TAS}^2 S} \tag{12}$$

The drag polar consists of two main parameters: the zero-lift drag coefficient C_{D_0} and the induced drag C_{D_i}, which is equal to kC_L^2. Together, they can be used to determine C_D according to Equation 13 obtained from Anderson.[28]

$$C_D = C_{D_0} + C_{D_i} = C_{D_0} + kC_L^2 \tag{13}$$

For some special flight strategies, such as maximum range or maximum performance it can be shown that there is fixed relation between C_{D_0} and C_{D_i}.[28] In this method it is assumed that aircraft in cruise will fly at at maximum range strategy. This strategy allows to fly as far as possible with the minimum amount of fuel. This strategy leads to the following relation.

$$C_{D_0} = 3C_{D_i} \tag{14}$$

Using this relation and C_D both parameters can be determined and a full drag polar can be generated.

The last method to determine C_D is using descending phases. Most commercial airliners reduce the thrust to idle during descent to save fuel. By assuming that the aircraft maintains a glide path angle for maximum range, to optimize fuel use, leads to the aircraft flying at its optimal lift over drag ratio. From Anderson[28] a simple relation between glide path and lift over drag ratio during descent is obtained, which is given in Equation 15.

$$tan(\gamma) = \frac{1}{L/D} = \frac{1}{C_L/C_D} \tag{15}$$

Combining Equation 15, the lift equation from Anderson[28] and the assumption that this is a steady descent, meaning $L = W cos(\gamma)$, Equation 16 is obtained.

$$C_D = \frac{W cos(\gamma)}{0.5 \rho S V_\infty^2} tan(\gamma) \tag{16}$$

Similar to the cruise phase it is possible to determine the drag polar for the descending phases. It can be shown that during the maximum range strategy in descent C_{D_0} and C_{D_i} are equal. Using this knowledge and the determined C_D the drag polar can be determined.

So far the method has described the calculations and assumptions needed to determine the parameters. But it was not yet shown how this is implemented. Next the implementation is discussed.

II.B.4. Statistics

For every measured parameter a statistic is maintained. Every measurement is binned, the mean is calculated and standard deviation is updated. To cut on memory usage the previous values are not stored. This means that the mean and standard deviation need to be updated. This is done using Equation 17 and 18 obtained from Dekking[29]

$$\mu_{i+1} = \frac{N_i \mu_i + X_{i+1}}{N_{i+1}} \tag{17}$$

$$\sigma_{i+1} = \sqrt{\frac{N_i \sigma_i^2 + (X_{i+1} - \mu_{i+1})^2}{N_{i+1}}} \tag{18}$$

Here N_i is the counter that tracks the number of measurements added, μ_i is the mean, X_i is the value of the random variable and σ_i is the standard deviation.

The maximum and minimum are updated by checking if the new value is larger or smaller than the current maximum or minimum. When a value is larger than the current maximum this value is set as the maximum. A value larger than three times the standard deviation is ignored. This limit is introduced to make sure that the minimum or maximum will not be set by noise.

II.C. Implementation

The amount of data that needs to be processed in this method is larger than most computers can handle in their memory. Therefore the following method was chosen to make processing of this data possible on normal machines, without large amounts of available system memory. In Figure 3 an overview of the implementation can be seen.

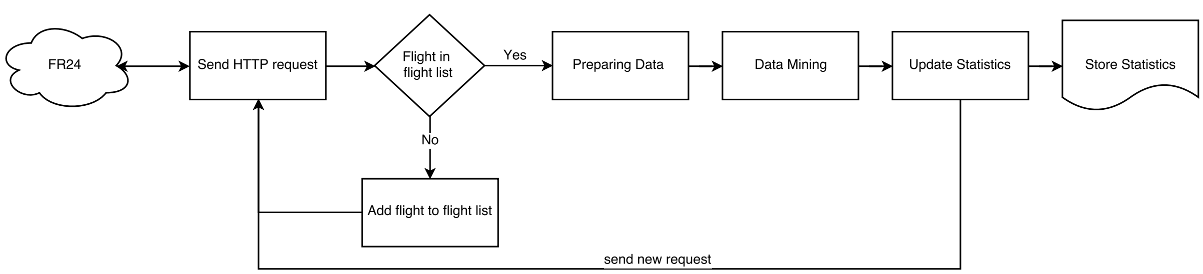

Figure 3. Flow chart of APE tool

The main idea behind the implementation is on-line processing. Meaning that when a measurement is obtained it is directly processed. This circumvents the need for large storage. For every measurement obtained from Flightradar24 the steps in Figure 4 are performed.

First the measurement variables are updated. Then they are filtered. In this study only the acceleration is smoothened. Next the state of the flight is updated and the phase is determined using fuzzy logic. Depending on the phase the methods discussed earlier are applied to calculate W, C_L , C_D,, C_{D_0} and C_{D_i}. Finally the statistics are updated.

When a flight is finished it needs to be removed from memory, but occasionally a measurement is missing. Therefore a distinction needs to be made between missing flights and finished flights. Depending on the phase

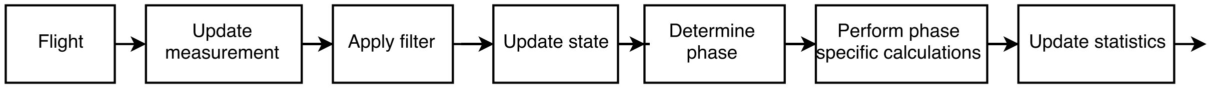

Figure 4. Flow chart of inner functions of the APE tool

and state of the last measurement the program waits either 20 minutes or 3 hours before deleting the flight object. The 3 hours is necessary for trans-Atlantic flights, where it is common that aircraft go unobserved for a few hours. A more detailed description of the implementation is given in the Appendix.

II.D. Evaluation

At this point the method produced statistical information on the parameters of interest. Next these values need to be verified and the method validated. Because there is only limited actual comparable data publicly available. The flight envelope parameters are compared to public data on manufacturers websites and trusted instances. For this mainly the Eurocontrol Aircraft Performance Database (EPD)[30] is used. The drag polar is compared to BADA. Since the BADA data is proprietary only the maximum differences are shown. Finally the parameters are used to perform a simulation. For this simulation a simple point mass model is made. Next the ground speed, rate of climb and flight path angle measurements from a flight are taken and used as input for the model. The resulting output parameters are inspected and discussed.

III. Results

Now that the method has been explained, the results can be discussed. The results are illustrated in detail using the analysis of a B737-800. The B737-800 is used because it is one of the most used commercial aircraft types. This made it possible to analyze thousands of flights in a matter of hours. The results shown in this section are obtained by measuring all B737-800 flights world wide for almost 16 hours. The data includes over 11.000 flights and over 11 million ADS-B measurements. First the results for the operational flight envelope are presented and secondly the lift and drag coefficients are discussed. Other aircraft types, such as A320, B787-800 and the A380, are also discussed, but the results are shown in a more compact manner.

III.A. Operational Flight Envelope

The results are observations obtained from the ADS-B measurements. In Table 1 the most important parameters and phases are shown for the B737-800. This table shows the mean and standard deviation from the measurements for important variables and phases. The full results for the operational flight envelope calculations can be seen in Table 3 in the Appendix. Also the full results for the A320, B787-800 and A380 are given in the Appendix.

Table 1. Most important results for B737-800

Parameter	Ground		Climb				Cruise		Descent					
	μ_{TO}	σ_{TO}	μ_{IC}	σ_{IC}	μ_{CL}	σ_{CL}	μ_{CR}	σ_{CR}	μ_{ID}	σ_{ID}	μ_{D}	σ_{D}	μ_{FA}	σ_{FA}
V_{TAS}	58.66	16.71	95.51	13.92	183.74	33.64	229.1	23.51	222.76	24.15	158.44	33.0	83.68	14.55
$\dot{V}_{TAS}$	2.04	0.76	0.39	1.0	0.17	0.49	0.0	0.32	-0.05	0.42	-0.1	0.41	-0.1	0.33
h	0	0	652	288	5034	2110	10781	1007	9162	1324	3872	1712	607	315
$\frac{dh}{dt}$	0.0	0.0	10.38	4.35	11.42	4.26	0.01	0.26	-8.66	4.84	-7.12	3.28	-4.11	1.29
M	0.17	0.05	0.28	0.04	0.58	0.12	0.77	0.08	0.74	0.08	0.49	0.11	0.25	0.04
γ	0.0	0.0	0.11	0.05	0.07	0.03	0.0	0.0	-0.04	0.02	-0.04	0.02	-0.05	0.01
ϕ	0.0	0.0-	0.15	0.68	0.09	0.83	0.03	0.81	0.04	0.76	0.07	0.63	0.07	0.5
$\dot{E}$	0.0	0.0	135.53	122.48	139.42	168.24	0.31	80.31	-97.08	164.56	-86.65	176.22	-49.1	45.95

To give some reference the results are compared to the performance figures obtained from the EPD.[30] In

Table 10 the performance of a B737-800, obtained from the EPD, can be seen. Similar tables for the A320, B787-800 and A380 are given in the Appendix.

Table 2. Flight performance of B737-800 obtained from Eurocontrol Aircraft Database[30]

Parameter	Take-off	Initial Climb	Climb	Cruise	Initial Descent	Descent	Approach	Landing
$V_{TAS}(m/s)$	75	85	150	237	-	145	128	75
$h(m)$	0	1525	4570	12500	8000	3000	-	0
$\frac{dh}{dt}(m/s)$	0	15	10	0	-4	-17	-8	0
M	-	-	-	0.79	0.78	-	-	-

The Lets start by looking at the true air speed, since this will have much influence on the other phases. The average speed during take-off is 58 m/s. This should not be confused with the lift-off speed. The estimated lift-off speed is 73.14 m/s. According to the EPD[30] the lift-off speed for the B737-800 is around 75 m/s, which is virtually equal to the estimation. In Figure 5 a comparison is made between EPD and the results for four aircraft types. The first column shows the take-off phase. Here the average true air speed for take-off, lift-off and EPD are shown. As expected the average take-off speed is lower than the lift-off speed. The speed given by the EPD is the lift-off speed and is very close to the lift-off speed measured. For all aircraft the lift-off speed given by EPD is within one standard deviation from the mean.

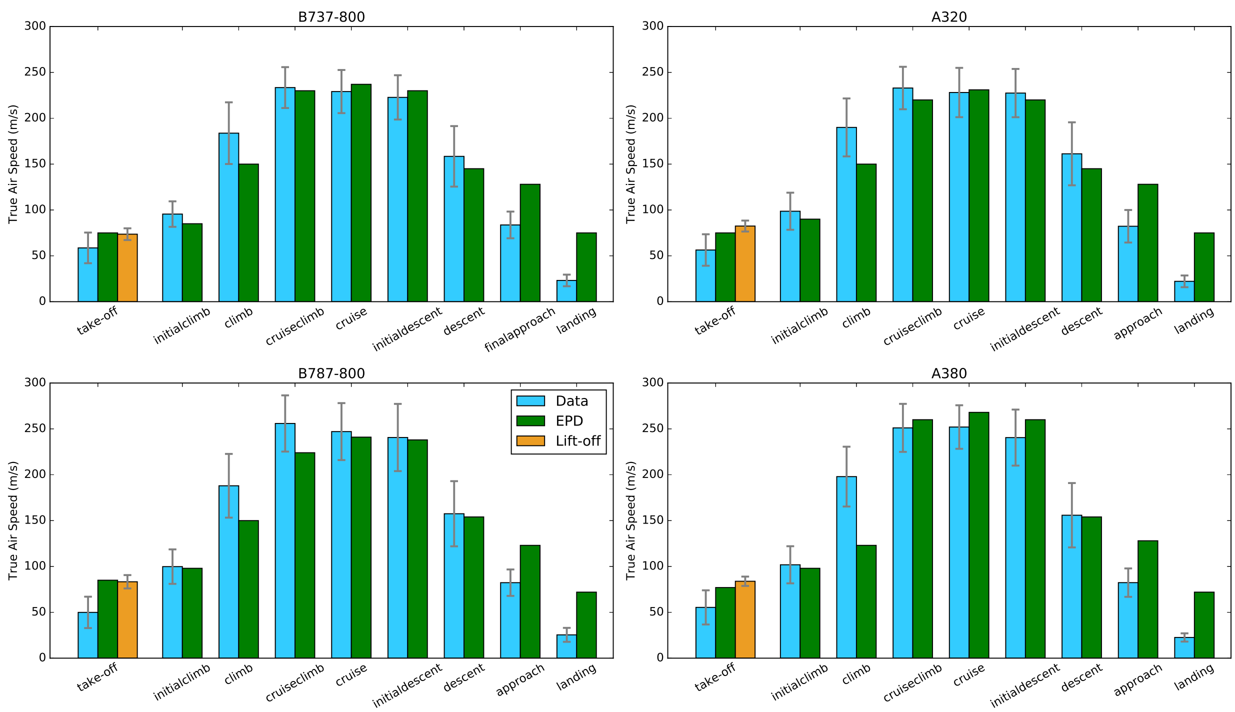

Figure 5. Comparison of measured true air speed against Eurocontrol Aircraft Database

Figure 5 shows that the results are similar to the reference data for most phases. For example the cruise speed differs only slightly for all aircraft and the reference data is within one standard deviation from the mean. The phases that differ most are the climb, approach and landing. There are multiple causes that influence the measurement, which might result in a difference. First there are the phase definitions. The phase definitions are comparable, but not exactly the same as the EPD definitions. In this research the measurements are classified based on lift configuration. This causes the climb phase to start at lower altitude than in the EPD. Also the final approach phase starts at lower altitude than in the EPD, therefore the aircraft has decelerated more before landing. The landing phase also shows large difference. This is mainly caused by bad classification. Measurements taken during landing are filtered by determining the moving average. This causes many of the first measurements during landing to be identified as final approach, because previous measurements taken into account. Only measurements late into the landing are classified as landing, which leads to a low landing speed. The landing is not used for any further analysis, therefore nothing has been done to change this behavior. Another interesting point to notice is the true air speed for cruise climb. This speed appears to be larger than the cruise speed. A possible cause could be a climb strategy that some airlines use. When the aircraft is close to cruise altitude the thrust is reduced and the obtained momentum is used to reach final cruise altitude and thus exchanging speed for altitude.

It is also possible to compare the Mach number, which are given in Tables 1 and 10. The measured average Mach number is 0.77. According to Boeing[31] the Mach number at zero wind flight and at cost index zero is 0.773 for a B737-800. Most airlines would fly at cost indexes around 12,[32] making the Mach number of 0.78 given by the EPD plausible.

For both the true air speed as the Mach number, the measured values are close to the reference data. This builds confidence in the method, but also of the assumption that wind will cancel out due to the large number of measurements.

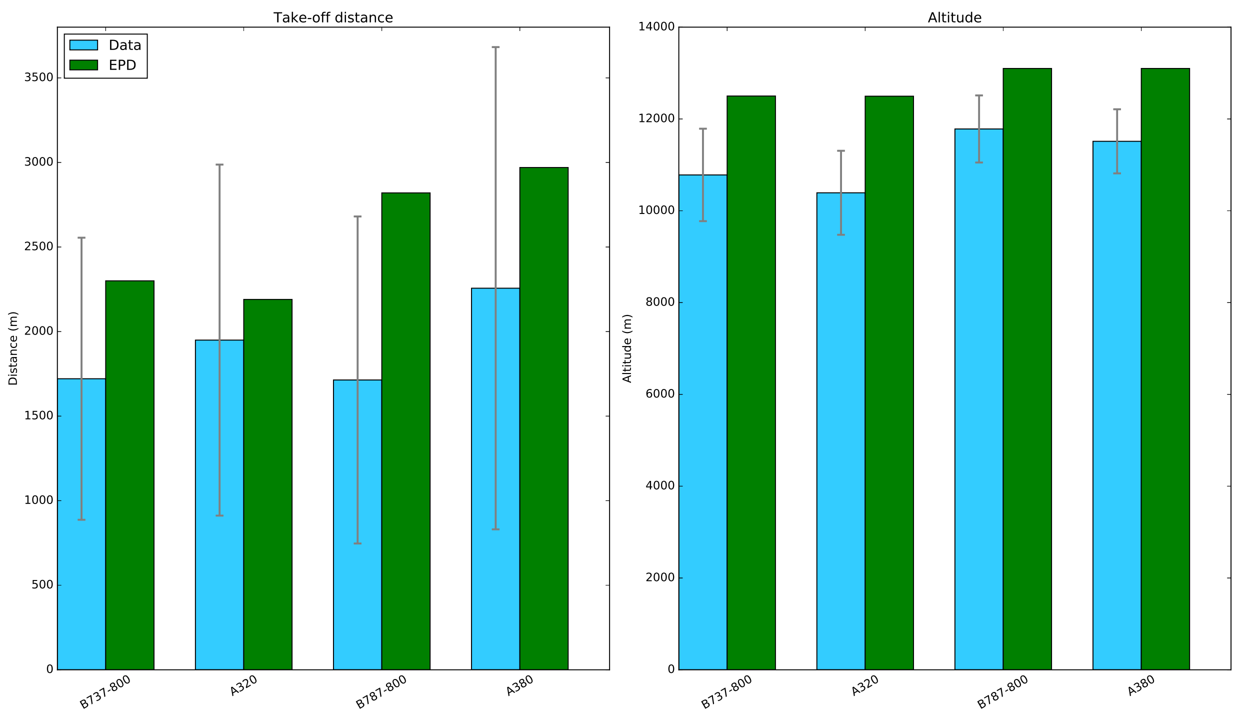

Figure 6. Comparison of take-off distance and cruise altitude

The take-off distance is the major parameter on which the take-off weight is based and therefore important for many of the calculations performed in this study. In Figure 6 a comparison is made of the measured take-off distance and the EPD. For all aircraft types the mean take-off distance is significantly lower than the EPD data. Also the standard deviation for these parameters is large. This leads us to believe that the measurement is noisy. The number of measurements belonging to take-off are small. The temporal resolution is around 5 seconds, therefore a maximum of only 5 or 6 measurements per flight are taken. This also means that when one measurement is missing a large portion of the distance is not taken into account. There are multiple reasons why a measurement could be missing. First there is the ADS-B coverage. Take-off is on the ground and therefore it is more likely that buildings and trees are blocking ADS-B antennas reducing the coverage of the system. Secondly the classification is difficult, by using a moving average it might happen that the measurements at the start of take-off are wrongfully classified. At the other end of this spectrum, measurements that actually should be part of the initial climb are assigned to take-off. This could explain the standard deviation to be so large. A possible solution to this would be to change the filtering method. Also different classification methods could be used to find the best option. For the weight estimation it becomes clear that not one parameter should be used. Other parameters such as lift-off speed could also be used.

On the right of Figure 6 the cruise altitude is compared with EPD. It should be noted that the altitude given by the EPD is actually the maximum rated altitude for the corresponding aircraft type. Therefore it is to be expected that the measurements show a lower cruise altitude. Even when one standard deviation is added to the mean the altitude is lower than the EPD. This builds confidence since in reality almost no aircraft would fly close to the rated maximum altitude. The altitude for the individual phases are less important since they are largely defined by the fuzzy logic parameters set in the method.

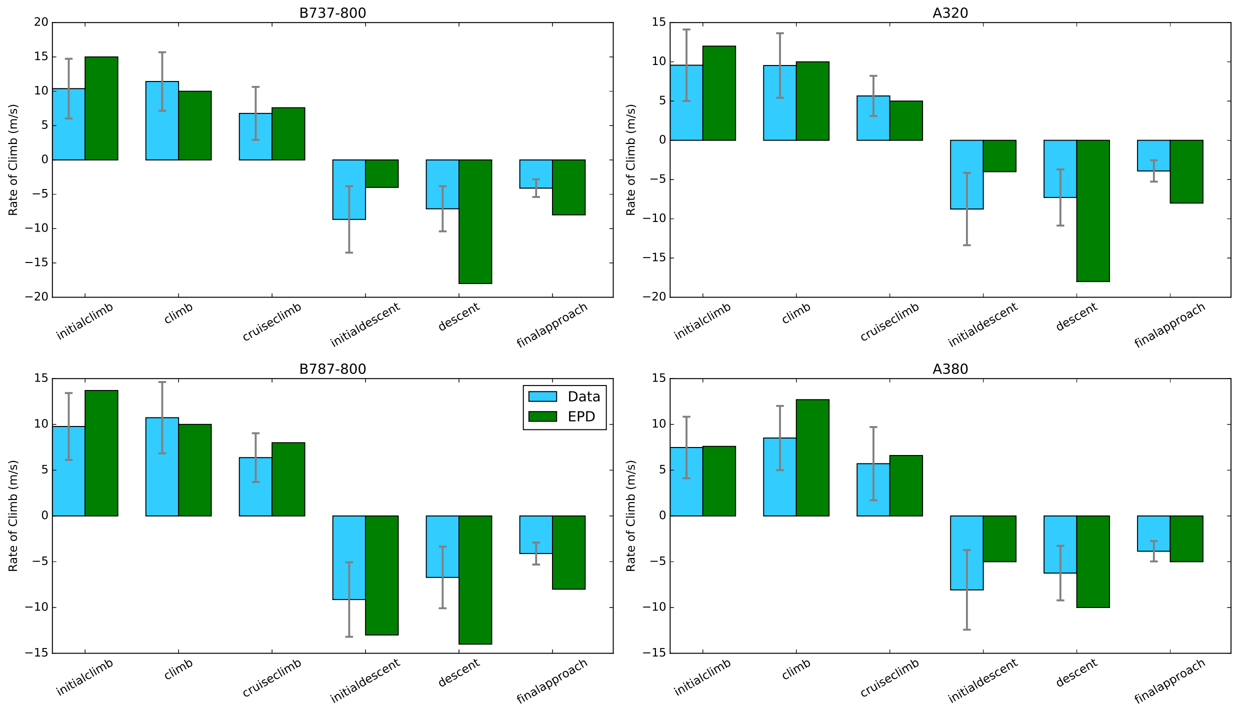

Figure 7. Comparison of measured rate of climb against Eurocontrol Aircraft Performance Database

The climb and descent performance is next to the speed and altitude and important part of the flight envelope. In Figure 7 the climb and descent performance for different aircraft types is shown and compared to the EPD. In general the rate of climb during the initial climb is lower. This could be caused by the slight differences in phase definition. The values for climb and cruise climb are close and within standard deviation. For the initial descent a difference can be seen by the short range and long range aircraft. It should be noted that the EPD is for educational purposes and no indication whether the data is a maximum or average is given. For the previous parameters it was clear from the values, but for the climb performance this is less apparent. An interesting difference to note is the envelope of climb and descent. Where the EPD expects a decreasing rate of climb, the measurements show that an aircraft will increase its rate of climb during the climb phase. A similar difference can be seen during descent. The lack of context on the EPD data makes it difficult to pin point a probable cause. This is also visualized in Figure 8. Here the flight envelope from the measured data is plotted against the EPD data.

The other parameters such as $\dot{V}_{TAS}$, γ and ϕ are not given by the EPD. A short inspection of these parameters is given. The acceleration $\dot{V}_{TAS}$ is rather low during the flight. This is expected, since high accelerations degrade the user comfort. A clear positive acceleration can be seen during take-off. No information on γ could be found from another trusted source, but there is one phase where γ is widely known. This is the final approach. Here the aircraft follows the Instrument Landing System (ILS) glide-slope which is around -0.0524 rad (-3 degrees). This is very close to the γ found in the measurements. This provides confidence that the method used and the other measurements are correct as well. For the bank angle ϕ no specific optimal performance parameters were found, only limits were found. From the Boeing Technical Guide[33] it was found that the limit on bank angle is set to $\pm$ 0.5 rad. The average of the measured ϕ is definitely within the limits, but the standard deviation on the parameter is large. This could be caused by the noise, since ϕ is based on the time derivative of the heading.

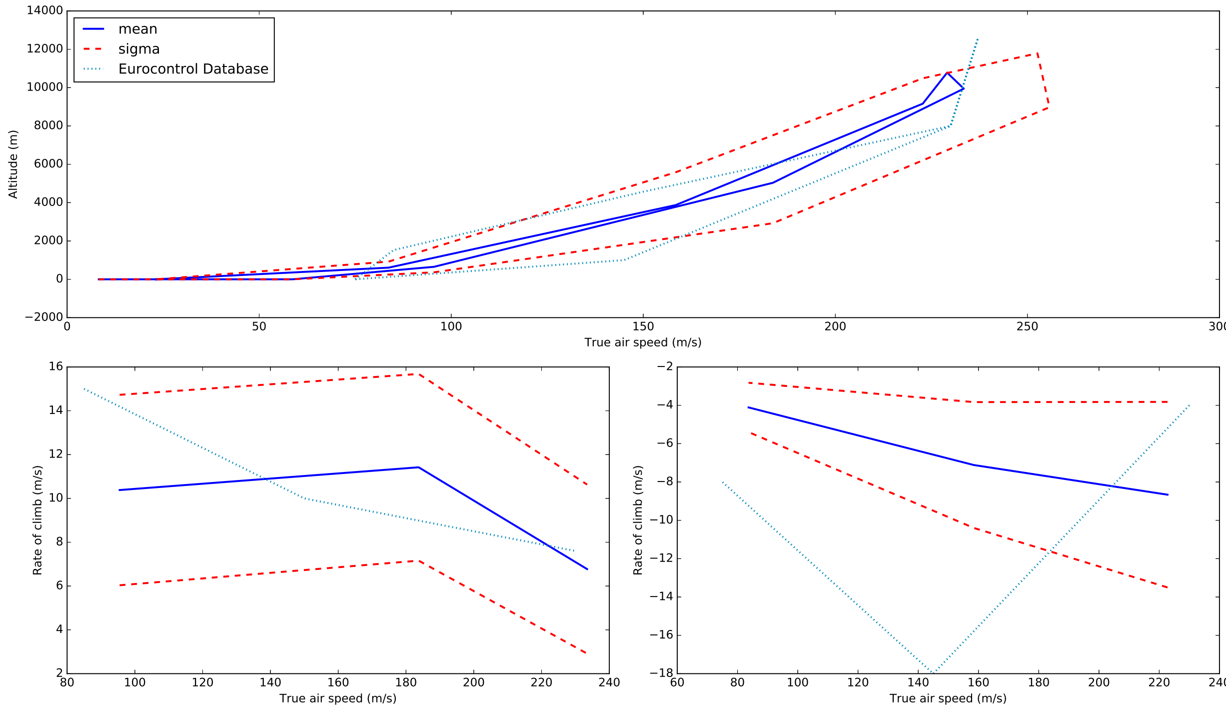

Figure 8. Flight envelope B737-800

III.B. Lift and Drag Coefficients

In this study multiple methods are proposed to determine the lift- and drag coefficients and the corresponding drag polar for climbing, cruising and descending phases. The method for the climbing phases turns out to be very unreliable. This is due to the fact that $\dot{V}_{TAS}$ is very noisy and sometimes becomes zero. Since the method divides by $\dot{V}_{TAS}$ this will mean that C_D will become infinite, when $\dot{V}_{TAS}$ is zero. Efforts to suppress or filter this behavior turned out unsuccessful. Even when a proper mean was found the standard deviation would be an order too large due to the noise. For on-line analysis this method is too sensitive for noise. But for offline analysis, where filtering options can be more elaborate, this method might work. Even then there is no method to determine C_{D_0} and K. The results for the cruise and descending phases are shown in Figure 9.

Looking at C_L the pattern makes sense from a flight mechanics perspective. During initial climb C_L is around 1.09 after which it starts to decrease to around 0.4 when the aircraft accelerates and changes its configuration and angle of attack. Due to a positive flight path angle the thrust is aiding in overcoming the gravity. This is what causes the increase in C_L during the cruise phase. The mean C_L remains similar until final approach is started. Here the configuration is changed to allow flight at lower speeds.

The remaining plots show the distribution of C_D, C_{D_0} and K for the cruise, initial descent, descent and final approach phase. The first thing that stands out is the C_D during cruise. The graph shows a negative minimum. The reason that this is possible is because C_D is determined based on ΔW. Because of the noise in the data it sometimes happens that ΔW becomes positive, where a decrease in weight is expected. This could cause the C_D to be negative. It would be possible to just remove the negative values, but this is not done for the following reason. The idea behind the method is to use the trend in the ΔW signal to determine C_D. The actual ΔW fluctuates around this trend line. This is not a problem as long the trend in the signal is negative. By removing the negative values from the signal the trend of the signal is altered, which in turn causes a change in the resulted C_D. In order to see the implications of that change a test run was preformed where the negative values where filtered out. The resulting C_D turned out to be a factor 7 too large. Therefore a choice was made not to remove the negative C_D values.

For the descending phases the distributions are reasonably normal distributed. The median (red stripe) is fairly close to the mean (black dot). But for the cruise the distribution is skewed. The median is very close to the first quantile. This is probably caused by the previously discussed negative C_D.

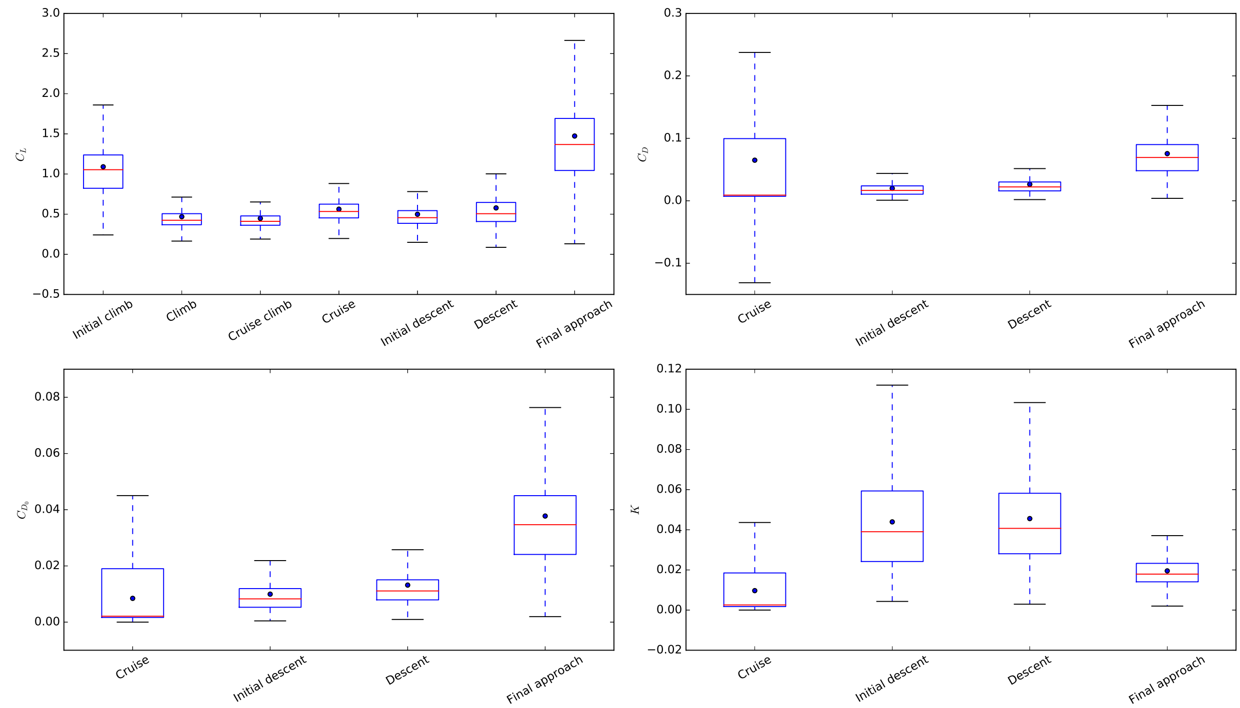

Figure 9. Boxplot for C_L and C_D

The drag polar of the aircraft is not known. Therefore it is not possible to validate the numbers for C_D. In order to give some indication on the quality of the results, they are compared to BADA. Since also the BADA drag polar data are proprietary only the difference with BADA is presented. BADA provides 5 different drag polars for different flap settings. From the ADS-B data it is not possible to determine what the configuration of the aircraft is. However for some phases of flight it is known what configuration the aircraft is in. For example an aircraft in cruise will generally always fly in clean configuration. Also an aircraft in final approach will have a high lift configuration to make sure the landing speed is low enough. Using this knowledge it is possible to assign a configuration to a phase. Here the clean configuration is assigned to the cruise, initial descent and descent phases. A high lift configuration is assigned to the final approach.

In Figure 10 the comparison with BADA is shown. For every phase a plot is made where the maximum difference between the measured drag polar and BADA is plotted. The maximum difference is determined for a predefined operating lift coefficient range of $0.4 - 0.8$ for the clean configuration phases. The lift coefficient range used for the high lift configuration is $0.8 - 1.8$.

Two measured drag polars are compared. The first is the mean drag polar, which is made by using the mean $\mu_{C_{D_0}}$ and μ_K. Let us refer to this drag polar as Q_1. The second drag polar is made by using $\mu_{C_{D_0}} + \sigma_{C_{D_0}}$ and $\mu_K + \sigma_K$, this one is called Q_2. The comparison is made for four aircraft types. The results in Figure 10 show that the maximum difference between BADA and the measured drag polars is larger for Q_1 and becomes smaller by adding the standard deviation. Only for long range aircraft during initial descent and descent this does not hold. There Q_1 shows a smaller error from BADA. For the cruise phase two possible explanations could exist. First it is possible that the thrust specific fuel consumption used was not exactly correct. Secondly it is possible that the assumption, that aircraft flies at a maximum range strategy, does not hold. This would cause the relation between the zero-lift drag coefficient and the induced drag coefficient to be different. More likely the error is caused by a combination of assumptions and noisy data. For the descending phases the maximum difference between Q_1 and Q_2 is smaller. For the final approach, where the aircraft is known to have a high lift configuration the maximum difference becomes larger again. Again this is probably because the actual flight strategy is different from the one assumed in the method.

So far we have looked at the maximum difference in C_D between Q_1 and Q_2 for a range of possible C_L, but it is more interesting to know the difference at the mean operating C_L, since this is where the aircraft is

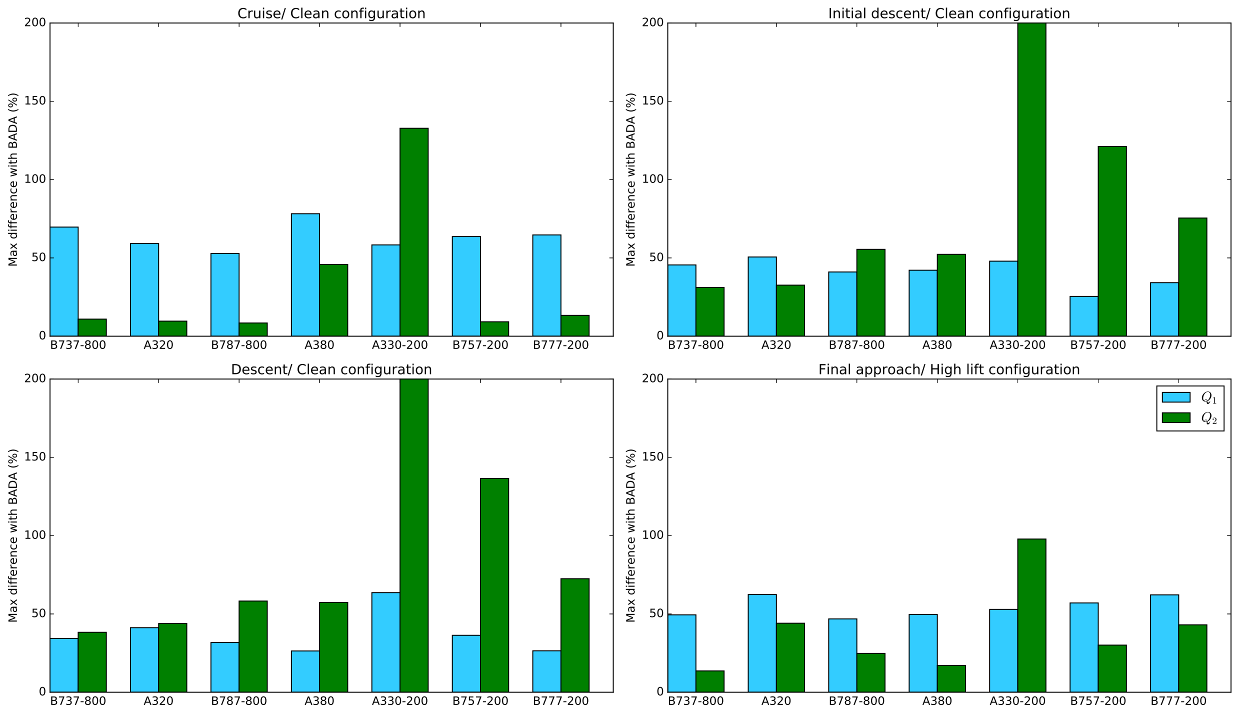

Figure 10. Maximum difference of data with BADA within the operational lift coefficient range

more likely to operate. This is shown in Figure 11. These results amplify the previous results, because the difference with Q_1 and BADA is significantly larger at the mean operating lift coefficient than Q_2. Overall the differences at the mean operating point for Q_2 are very low. This is consistently the case for multiple aircraft types. This gives the impression that the method currently underestimates the drag polar.

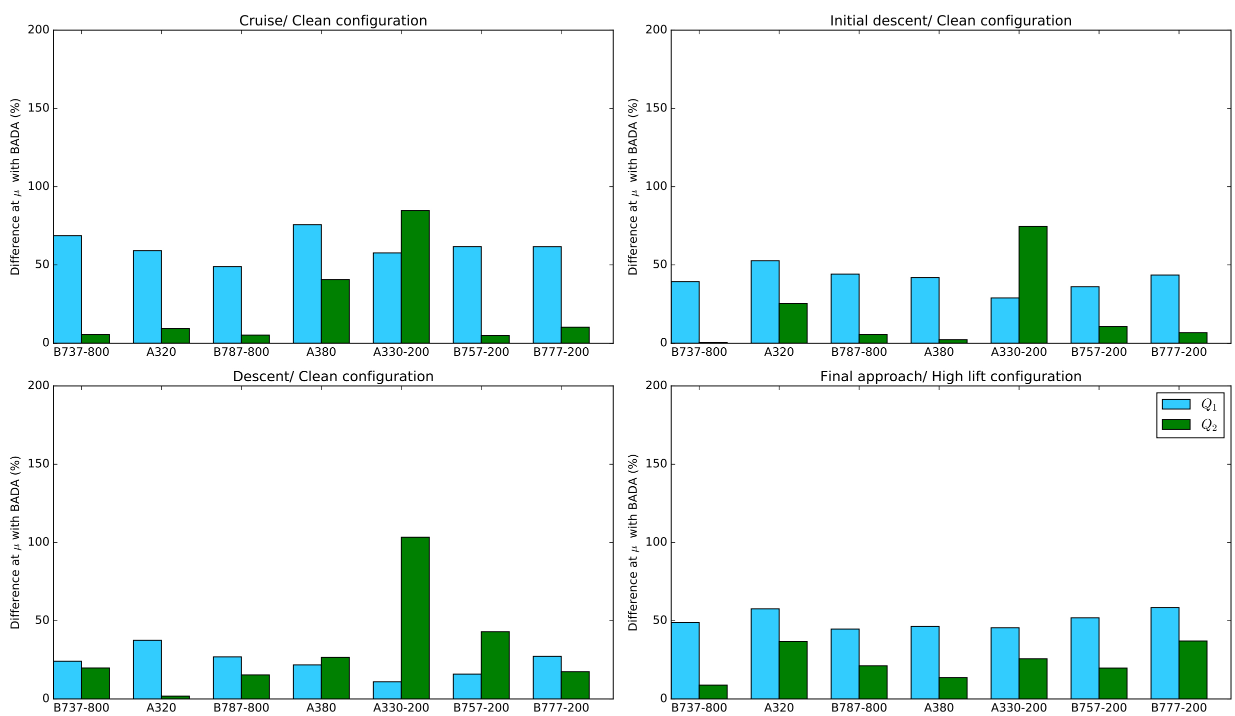

Figure 11. Difference of data with BADA at the operational lift coefficient

The previous figures all show the absolute difference with BADA for specific aircraft types. Next we combine differences for all the aircraft types an look at the resulting statistics. In Figure 12 statistics on the difference with BADA for different phases are shown. Again it can be seen that the overall difference for Q_1 is larger in the cruise phase. Q_2 is even very close to zero, but a slight increase in spread can be seen. This increase in spread is much larger for the initial descent and descent phases. Also the overall difference is larger for Q_2 is those phases and interesting to see is the switch from a negative error to a positive error. For the final approach phase, the spread is smaller again. As was seen before the difference with BADA for Q_1 is larger than Q_2. Figure 12 clearly shows that the method used in this study estimates a lower drag than BADA would in all phases. By adding one standard deviation a result more similar to BADA is obtained. But it should be noted that BADA is not equal to the actual drag polar as well.

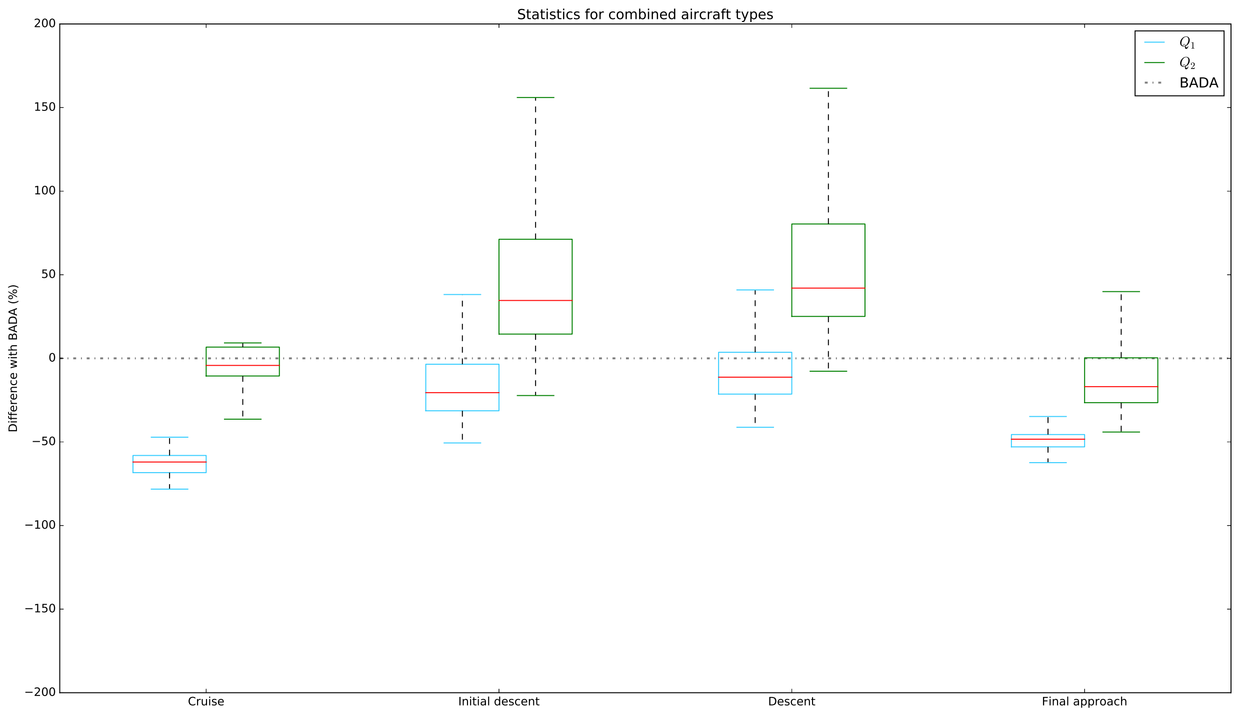

Figure 12. Error statistics of the comparison with BADA.

III.C. Simulation

So far the operational flight envelope is estimated and an estimation for the drag polar is obtained. To see how these newly found figures hold up during simulation a simple point mass model was made and a simulation was run.

The simulation is set up to recreate a measured flight. To achieve this ADS-B measurements are used as input to the model. The ground speed, rate of climb, flight path angle and corresponding aircraft type parameters are fed into the simulation. The resulting output includes thrust, drag, lift and weight forces. The non-symmetric parameters are obtained as well, but are not discussed here.

Two simulations are performed. The first simulation S_1 uses the drag polar Q_1 and the mean μ_{C_L}. The second simulation S_2 is done using drag polar Q_2 and $\mu_{C_L} + \sigma_{C_L}$. This extra comparison is done to rule out the possibility that the BADA drag polar data is not of high quality either.

The input data is obtained by measuring flight VA605 from Mackay Airport to Brisbane Airport on Saturday January 9. The first measurement was taken at 00:22:21 universal time and the flight took around 1.5 hours. The data is shown in Figure 13.

From Figure 13 it can be seen that the simulation correctly follows the input data. The altitude is not part of the input parameters, but the simulation is able to closely follow the measured altitude. There is some difference in the cruise altitude, which could be caused by the simple Euler method used for the numerical integration. The altitude is determined by numerical integration of the rate of climb. A different

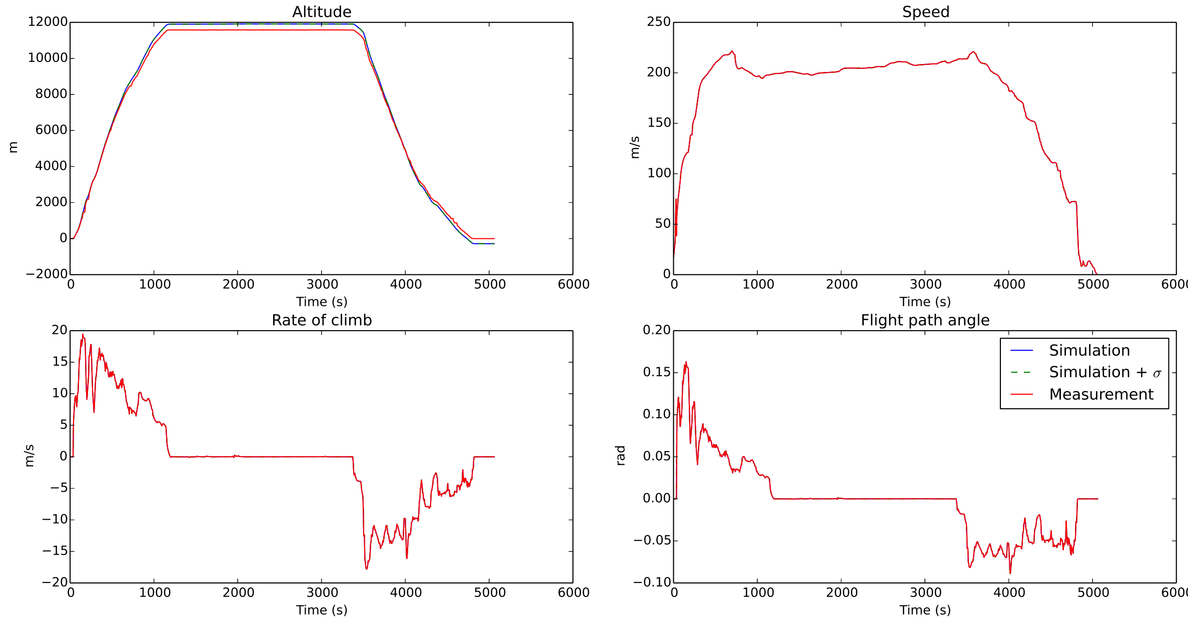

Figure 13. Simulation using measurement as input

method might make the error smaller. It is also possible that the difference exists because of noise in the input data.

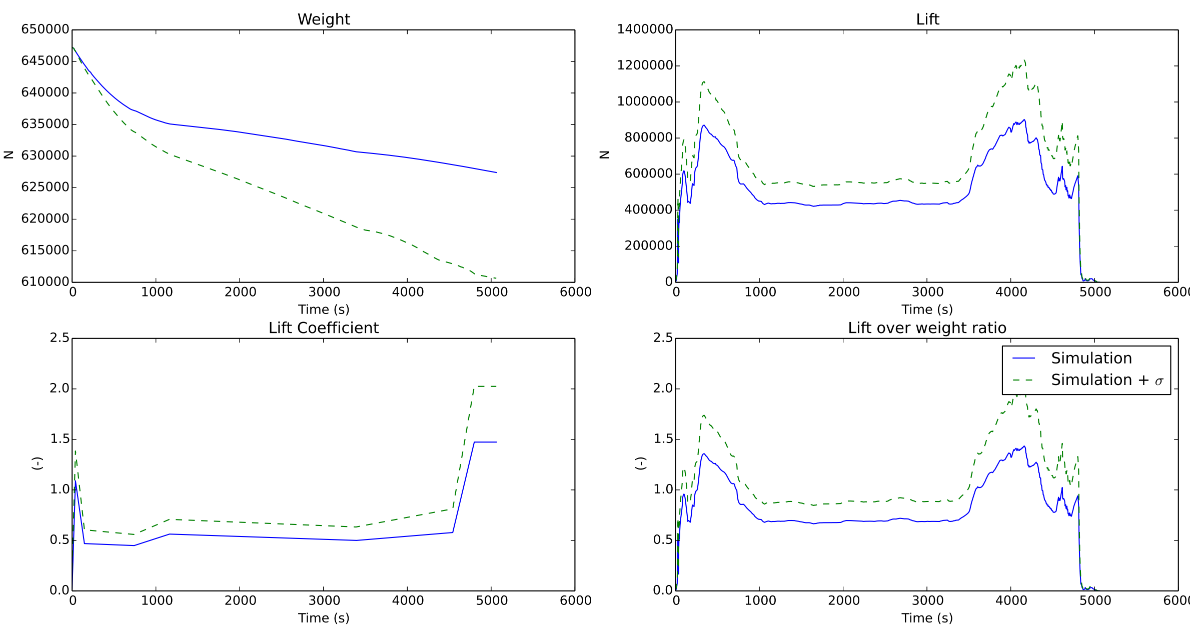

Figure 14. Simulation using measurement as input

One of the outputs of the simulation are the vertical forces. In Figure 14 four graphs are shown with the weight, lift, lift coefficient and the lift over weight ratio. The weight shows a large difference between the two different simulations. The increased drag causes the aircraft to use more fuel. The difference in fuel use is significant. This shows the importance of using the correct drag polar, because the difference in fuel use is large in only a short period of time.

More interesting to see in Figure 14 is the lift over weight ratio or load factor. It is understandable that the simulation is less accurate during the climbing and descending phases. Because it assumes steady flight, which is not necessarily the case. But what is interesting to see is the load factor during cruise. The assumption that the flight is steady during cruise is easily shown by the altitude and speed profile of the flight. Both are more or less constant during cruise. Therefore it is surprising to see that for S_1 the load factor is below one. This would mean the weight and lift are not in balance and some sort of acceleration would exist. The load factor for S_2 is much closer to one, but still slightly under.

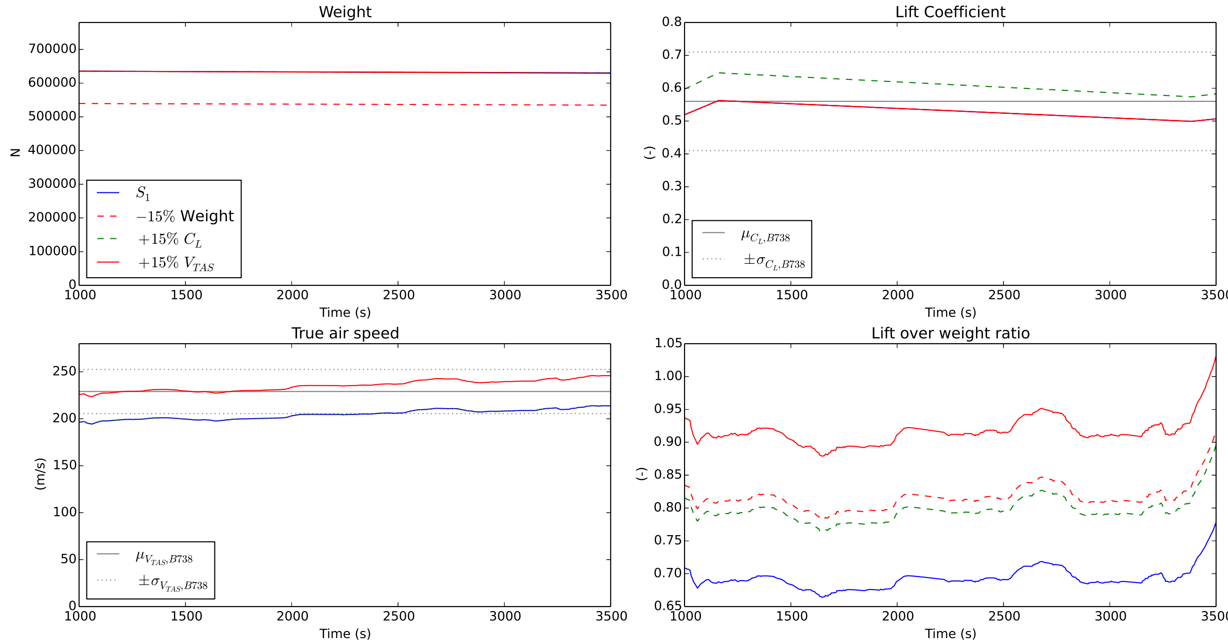

Figure 15. Sensitivity analysis of the lift-over-weight error

In Figure 15 an analysis is performed to expose the largest influences of this error. The three parameters on which the load factor depends are W, V_{TAS} and C_L. To determine the sensitivity of the load factor to changes in these parameters, all parameters are changed by 15% and plotted. From Figure 15 it can be seen that the load factor is most sensitive to changes in V_{TAS}. This is understandable because this relation is quadratic, where the relation of load factor with W and C_L is linear. Let us first cosider the true air speed used in the simulation. This is shown in the bottom left graph of Figure 15. In the figure the used cruise speeds are shown also the mean and standard deviation for cruise speeds of a B737-800 are shown. It can be seen that the speed in S_1 is approximately one σ smaller than the mean. This could actually be the case, but another possibility is the presence of wind. It could very well be that the aircraft encountered a head wind of around 30 m/s leading to a ground speed of approximately 200 m/s. This lower speed subsequently influences the lift calculation and thus the load factor. By adding 15% to the true air speed, which is approximately 30 m/s, the load factor becomes much closer to one. The remaining error is likely to be caused by both errors in W and C_L.

In Figure 16 the horizontal forces are shown. By increasing the drag polar also the drag and therefore the thrust need to be increased. This can be clearly seen. The question is which is a better estimation of the drag. Since the difference between drag and thrust during cruise is almost zero it is easier to look at the thrust values. Assuming a CFM56-7B24 engine is mounted the maximum cruise thrust per engine is 5,480 lbf (24376N) according to Jet-Engine.com.[27] This value seems plausible when compared to the values of older models, such as CFM56-3 engines which were used for the older B737 series. The values for the older models are published on the engine manufacturers website.[34]

Now comparing the simulated thrust to these values it is clear the S_1 shows very low thrust values and that S_2 is much closer to the cruise thrust given by the manufacturer.

This simulation shows similar findings as the comparison with BADA. Simulation S_2 shows more realistic values, which is caused by better aerodynamic coefficients.

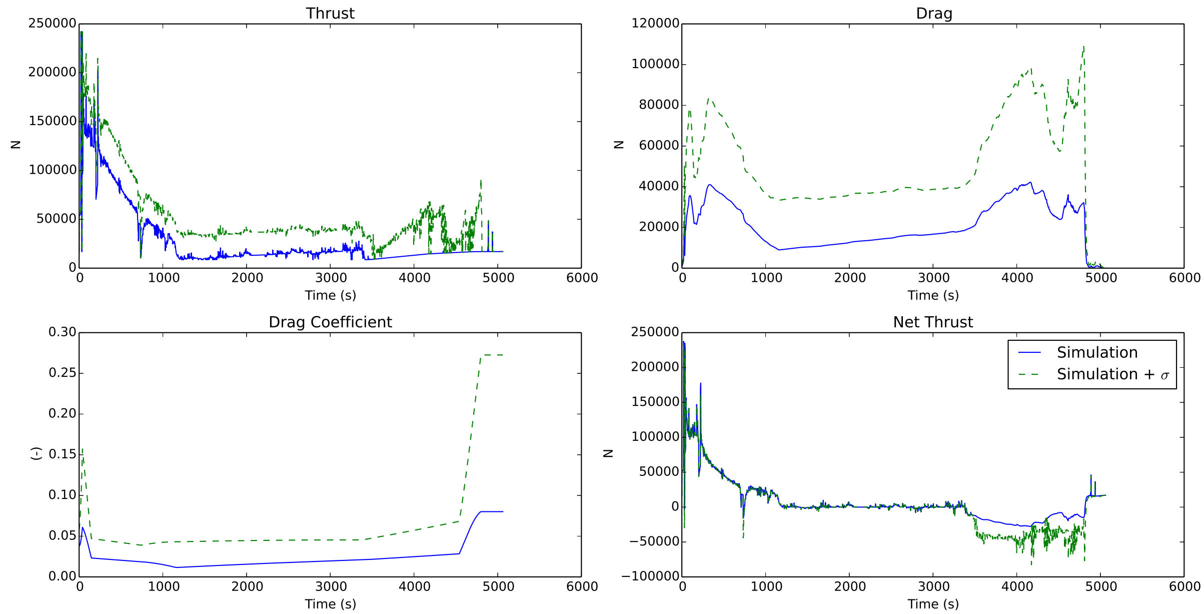

Figure 16. Simulation using measurement as input

IV. Discussion

So far a method and results are shown for this research. The goal was to find the operational flight envelope and to estimate lift and drag coefficients using ADS-B data. The use of global ADS-B data offers a lot of information and so far little research has been performed using this information.

A straightforward method is proposed to estimate the operational envelope, by simply taking measurements. But there are a few drawbacks to this method. The first drawback is that ADS-B data only provides ground speed. To determine the true air speed it is assumed that on average the effects of wind speed and direction cancel out. For the V_{TAS} was shown that this assumption gives good results when compared to the Eurocontrol Aircraft Performance Database. Although the standard deviation could be reduced by taking wind estimations into account. In some occasions supersonic ground speeds were measured, because the aircraft had a large tail wind. This is beyond the maximum speed of a B737-800. Implementation of wind speed and direction is possible by using the GFS predictions.

In order to determine the weight the take-off distance was determined and used to estimate the payload weight. The estimated take-off distance was lower than the EPD for all aircraft types. Also the standard deviation was large. This is probably caused by miss-classified measurements, noisy data and low resolution of the measurements. It was shown that it is possible to isolate ADS-B measurements that belong to the take-off phase based on acceleration. Because of the noise in the data is was necessary to filter the acceleration, which was done by using a moving average. This filtering method did not have a perfect score on phase classification. Also the low temporal resolution made the influence of missing measurement large.

This result for the take-off distance shows that using only the take-off distance for weight estimation is not enough. This method is used for its simplicity. It was never the goal of this research was to develop a full working method for take-off weight estimation. By only determining the payload weight using take-off distance the influence on the weight was limited. Many other variables are in play during take-off, such as thrust settings, wind and flap settings. A combination of these parameters will be necessary to develop a better weight estimation method.

The rate of climb was compared to EPD, which in values were pretty close. The major difference was the envelope. The EPD expected the rate of climb to decrease with increasing altitude. This was not the case for most aircraft. Only for the A380 this pattern was similar. The missing context on these EPD values makes it difficult to state a cause for the differences.

Next a method was given to determine the lift- and drag coefficients. This method implements a combination of ADS-B measurements, ADS-B derivatives and assumptions. In order to determine the C_D during climb the change in excess thrust was used. Even though the method seemed plausible in preliminary work, the method did not work well in practice. The noise in the acceleration signal is too large. The method is better suited for offline analysis, where it is possible to use different filtering techniques.

The C_D and the corresponding drag polar that was found for the other phases looks much more promising. By comparing the results for multiple aircraft with BADA it can be seen that the method underestimates the drag. The comparison with BADA is important to get a sense of the quality of the estimation, but should not be seen as absolute reference. Since the drag polars from BADA are not the actual drag polars

To extend this sense of quality, the drag polars were tested using a simple simulation. The results of the simulation were similar as the comparison with BADA. The thrust in cruise using the found drag polar is much lower than values expected by manufacturers. Since the drag and thrust can be assumed to be in equilibrium during cruise, this leads to the conclusion that the drag is too low.

Another interesting results of the simulation was the low load factor during cruise. To find the origin of this low load factor, the sensitivity of the load factor to the three most important parameters was checked. It was found that errors in true air speed have the largest effect on the vertical force balance when recreating a flight from ADS-B data. The flight used had a cruise speed roughly 15% lower than the average determined earlier. Therefore the low true air speed was given as the main cause for the low load factor.

The most important finding is the underestimation of the drag polar. It is difficult to pin point the cause of this underestimation, since many assumptions are made in this method. Obtaining aerodynamic coefficients from ADS-B data has always been a long shot. In the end it was shown possible, with reasonable results. Determining the cause of the underestimation would greatly improve the method. To find the cause, potential causes should be eliminated systematically.

V. Conclusion

In order to build an open source APM, an effort was made to develop a method that could extract the operational flight envelope and possibly the lift- and drag coefficients from the large amount of samples available through ADS-B. For this purpose a tool was developed that can process aircraft ADS-B measurements in an on-line fashion. The method combines ADS-B data and makes assumptions on wind and flight strategy to determine the operation flight envelope. Also lift- and drag coefficients are determined.

Overall the tool can be used to find the operational flight envelope. In comparison with other open data the operational flight envelope results seem good. The assumption that the wind speed and direction cancel did not give any big problems. The true air speed compared well with the Eurocontrol aircraft database. Also other parameters such as rate of climb and altitude were as expected.

Next the lift- and drag coefficients were determined and compared with the BADA APM. The method underestimated the drag coefficients, where maximum differences of up to 200% were seen. The values at one standard deviation performed much better, with maximum differences for clean configuration as low as 10%. The drag polar was put to the test in a simple simulation. The results from the simulation and the comparison to BADA showed that the tool underestimates the drag polar.

VI. Recommendations

This research is a good start for exploiting the large amounts of ADS-B data available. The data still houses many more secrets that can be unveiled. This research maintained a more global approach with simple ideas and assumptions. This gives an inviting overview and insight into the problems and possibilities. The next step in this research would be to step away from the whole picture and to focus on small parts of the flight envelope. The most important parameter would be the weight estimation. The weight is crucial for many calculations and therefore should be properly estimated. Using only the take-off distance is not enough. Other parameters such as lift-off speed, rotation rate, lift-off acceleration, lift-off turn radius and lift-off flight path angle could be used to get a better estimation. The best approach here would be to get some reference data and use semi-supervised learning techniques. But when this is not available it might be possible to find patterns in the data by simply clustering the data. For example an aircraft with a short take-off distance a steep flight path angle and a high acceleration might be seen as a light aircraft. Another part of the weight estimation that could be improved is the fuel weight estimation. Airlines use standard tables and formulas to determine the fuel based on a few parameters such as weight and distance.

Another flaw in the current tool is the absence of wind. True air speed is one of the most important parameters in this analysis ans was shown in the simulation. Therefore it is important to have the best possible estimation. It is possible to implement wind estimations by using the GFS. The GFS provides atmospheric predictions every 6 hours at a resolution of 0.25 degrees. Using these predictions a better estimation of the true air speed can be made.

It is recommended to improve the phase classification methods. The fuzzy logic used in this study works very good for the larger phases. But for the short duration phases, where only a few measurement are available it is less good. Being able to classify individual measurements with great confidence is very valuable. Because many of the hidden knowledge is only revealed by rare occasions and few measurements. To be able to extract that knowledge you should be able to trust your methods. This also applies to filtering. In this research a simple moving average was used, but this is not good enough. Other on-line and off-line methods should be analyzed.

In the end the problem at hand is multi-parameter optimisation problem, with known constraints on many parameters. In this research no explicit use is made of these constraints. So maybe it is possible to use global optimisation strategies combined with simple models to minimize some specific cost function. Doing this for the whole flight envelope is difficult, but doing it in small steps could be a good approach. For example modeling the take-off and subsequently fitting the model to the data, might lead to better weight estimations. During take-off clear constraints exist on weight, lift coefficient, thrust and drag. Also weather data is widely available.

This research presented an overview and a guide. But subsequent research should be in-depth and focussed.

Appendix

Full results of multiple aircraft types

Table 3. Result statistics of B737-800

Phases		V_{TAS}	$\dot{V}_{TAS}$	h	$\frac{dh}{dt}$	C_L	C_D	$C_{D,0}$	K	M	γ	ϕ	dE
take-off	μ	58.66	2.04	0.0	0.0	-	-	-	-	0.17	0.0	-	0
	σ	16.71	0.76	0.11	0.08	-	-	-	-	0.05	0.0	-	0
	max	108.79	4.32	0.32	0.24	-	-	-	-	0.32	0.0	-	0
	min	8.52	-0.25	-0.32	-0.23	-	-	-	-	0.03	-0.0	-	0
initialclimb	μ	95.51	0.39	651.58	10.38	1.09	-	-	-	0.28	0.11	0.15	135.53
	σ	13.92	1.0	288.09	4.35	0.3	-	-	-	0.04	0.05	0.68	122.48
	max	137.26	3.37	1515.86	23.42	1.98	-	-	-	0.41	0.27	2.2	502.97
	min	53.77	-2.6	-212.7	-2.66	0.2	-	-	-	0.16	-0.05	-1.9	-231.9
climb	μ	183.74	0.17	5034.43	11.42	0.47	-	-	-	0.58	0.07	0.09	139.42
	σ	33.64	0.49	2109.8	4.26	0.14	-	-	-	0.12	0.03	0.83	168.24
	max	284.66	1.64	11363.82	24.2	0.88	-	-	-	0.93	0.16	2.57	644.15
	min	82.82	-1.3	-1294.96	-1.36	0.06	-	-	-	0.22	-0.03	-2.39	-365.32
cruise	μ	229.1	0.0	10780.75	0.01	0.56	0.065	0.01	0.01	0.77	0.0	0.03	0.31
	σ	23.51	0.32	1006.92	0.26	0.15	0.012	0.01	0.04	0.08	0.0	0.81	80.31
	max	299.64	0.97	13801.52	0.8	1.0	0.12	0.04	0.11	1.01	0.0	2.47	241.23
	min	158.57	-0.97	7759.98	-0.78	0.12	0	-0.03	-0.1	0.53	-0.0	-2.41	-240.61
initialdescent	μ	222.76	-0.05	9161.79	-8.66	0.5	0.02	0.01	0.04	0.74	-0.04	0.04	-97.08
	σ	24.15	0.42	1324.07	4.84	0.13	0.01	0.01	0.03	0.08	0.02	0.76	164.56
	max	295.23	1.21	13133.99	5.86	0.9	0.05	0.03	0.14	0.99	0.02	2.33	396.59
	min	150.3	-1.31	5189.59	-23.18	0.1	-0.01	-0.01	-0.05	0.48	-0.1	-2.25	-590.75
descent	μ	158.44	-0.1	3872.32	-7.12	0.58	0.03	0.01	0.05	0.49	-0.04	0.07	-86.65
	σ	33.0	0.41	1711.54	3.28	0.23	0.02	0.01	0.03	0.11	0.02	0.63	176.22
	max	257.45	1.14	9006.94	2.73	1.28	0.07	0.04	0.13	0.82	0.01	1.97	441.99
	min	59.44	-1.34	-1262.31	-16.96	-0.13	-0.02	-0.01	-0.03	0.16	-0.1	-1.83	-615.3
finalapproach	μ	83.68	-0.1	607.0	-4.11	1.47	0.08	0.04	0.02	0.25	-0.05	0.07	-49.1
	σ	14.55	0.33	315.25	1.29	0.55	0.04	0.02	0.03	0.04	0.01	0.5	45.95
	max	127.32	0.88	1552.74	-0.25	3.13	0.18	0.09	0.12	0.38	-0.01	1.56	88.74
	min	40.04	-1.08	-338.74	-7.97	-0.18	-0.03	-0.02	-0.08	0.12	-0.09	-1.43	-186.93

Table 4. Result statistics of A320

Phases		V_{TAS}	$\dot{V}_{TAS}$	h	$\frac{dh}{dt}$	C_L	C_D	$C_{D,0}$	K	M	γ	ϕ	$\dot{E}$
take-off	μ	56.347	2.125	0.042	-0.006	-	-	-	-	0.166	-0.0	-	0
	σ	17.181	0.827	0.566	0.274	-	-	-	-	0.05	0.004	-	0
	max	90.709	3.778	1.175	0.543	-	-	-	-	0.267	0.008	-	0
	min	21.986	0.471	-1.09	-0.555	-	-	-	-	0.065	-0.008	-	0
initialclimb	μ	98.621	0.386	826.628	9.568	1.011	-	-	-	0.293	0.102	0.129	131.425
	σ	20.212	0.782	354.81	4.552	0.377	-	-	-	0.061	0.054	0.584	108.213
	max	139.045	1.95	1536.248	18.673	1.765	-	-	-	0.414	0.21	1.296	347.852
	min	58.197	-1.178	117.009	0.464	0.256	-	-	-	0.171	-0.006	-1.039	-85.001
climb	μ	190.014	0.121	5332.59	9.529	0.408	-	-	-	0.598	0.054	0.054	111.773
	σ	31.595	0.789	1968.77	4.115	0.114	-	-	-	0.11	0.03	0.473	205.432
	max	253.203	1.7	9270.129	17.76	0.637	-	-	-	0.818	0.114	1.0	522.637
	min	126.825	-1.457	1395.051	1.298	0.179	-	-	-	0.378	-0.007	-0.893	-299.092
cruise	μ	228.058	0.014	10391.486	0.022	0.466	0.053	0.011	0.016	0.765	0.0	0.03	3.533
	σ	26.879	0.946	915.126	0.331	0.12	1.353	0.013	0.021	0.091	0.001	0.61	243.606
	max	281.816	1.907	12221.738	0.684	0.705	2.758	0.037	0.058	0.947	0.003	1.25	490.745
	min	174.301	-1.878	8561.234	-0.64	0.227	-2.652	-0.015	-0.026	0.583	-0.003	-1.19	-483.679
initialdescent	μ	227.448	-0.044	8921.888	-8.759	0.378	0.015	0.007	0.056	0.748	-0.039	0.032	-96.174
	σ	26.318	0.898	1212.19	4.611	0.101	0.008	0.004	0.033	0.09	0.02	0.442	260.875
	max	280.083	1.752	11346.268	0.463	0.579	0.031	0.015	0.122	0.928	0.002	0.916	425.576
	min	174.812	-1.84	6497.508	-17.98	0.176	-0.002	-0.001	-0.01	0.569	-0.079	-0.852	-617.924
descent	μ	161.242	-0.11	3861.564	-7.285	0.443	0.02	0.01	0.058	0.498	-0.045	0.052	-90.575
	σ	34.341	0.803	1684.88	3.582	0.165	0.012	0.006	0.033	0.114	0.019	0.573	207.514
	max	229.924	1.495	7231.324	-0.12	0.773	0.043	0.022	0.124	0.725	-0.007	1.198	324.452
	min	92.56	-1.716	491.803	-14.449	0.114	-0.003	-0.002	-0.007	0.27	-0.083	-1.094	-505.602
finalapproach	μ	82.239	-0.107	596.996	-3.906	1.228	0.061	0.031	0.022	0.243	-0.049	0.051	-47.565
	σ	17.738	0.465	313.207	1.361	0.434	0.029	0.015	0.011	0.053	0.015	0.335	53.732
	max	117.715	0.823	1223.411	-1.184	2.096	0.12	0.06	0.045	0.35	-0.019	0.721	59.899
	min	46.762	-1.037	-29.419	-6.628	0.359	0.003	0.001	-0.0	0.137	-0.078	-0.619	-155.028

Table 5. Result statistics of B787-800

Phases		V_{TAS}	$\dot{V}_{TAS}$	h	$\frac{dh}{dt}$	C_L	C_D	$C_{D,0}$	K	M	γ	ϕ	$\dot{E}$
take-off	μ	49.92	1.97	0.271	0.039	-	-	-	-	0.147	0.0	-	0
	σ	17.103	0.733	1.392	0.38	-	-	-	-	0.05	0.005	-	0
	max	84.127	3.437	3.054	0.799	-	-	-	-	0.247	0.011	-	0
	min	15.714	0.504	-2.512	-0.721	-	-	-	-	0.046	-0.01	-	0
initialclimb	μ	99.827	0.333	802.424	9.77	1.095	-	-	-	0.296	0.103	0.116	127.094
	σ	18.796	0.512	382.632	3.65	0.346	-	-	-	0.056	0.047	0.47	45.263
	max	137.419	1.357	1567.688	17.071	1.787	-	-	-	0.409	0.196	1.056	217.62
	min	62.234	-0.691	37.161	2.47	0.403	-	-	-	0.183	0.01	-0.824	36.567
climb	μ	187.963	0.161	4996.002	10.731	0.46	-	-	-	0.589	0.061	0.07	130.186
	σ	34.743	0.24	1970.996	3.896	0.149	-	-	-	0.119	0.029	0.49	53.419
	max	257.45	0.642	8937.993	18.522	0.759	-	-	-	0.828	0.118	1.049	237.024
	min	118.476	-0.319	1054.01	2.94	0.161	-	-	-	0.35	0.003	-0.91	23.347
cruise	μ	247.041	0.001	11782.189	-0.118	0.51	0.055	0.012	0.014	0.836	-0.0	0.025	0.23
	σ	31.056	0.159	730.911	0.247	0.204	1.178	0.013	0.016	0.105	0.001	0.605	40.012
	max	309.153	0.318	13244.011	0.375	0.917	2.41	0.038	0.046	1.047	0.002	1.235	80.254
	min	184.93	-0.317	10320.367	-0.611	0.103	-2.301	-0.013	-0.018	0.625	-0.003	-1.185	-79.794
initialdescent	μ	240.587	-0.061	9638.918	-9.132	0.369	0.014	0.007	0.057	0.798	-0.039	0.034	-103.082
	σ	36.65	0.255	1614.253	4.066	0.158	0.011	0.006	0.034	0.125	0.018	0.485	108.686
	max	313.888	0.448	12867.424	-0.999	0.685	0.037	0.018	0.124	1.049	-0.003	1.004	114.29
	min	167.287	-0.57	6410.412	-17.264	0.053	-0.008	-0.004	-0.011	0.547	-0.074	-0.937	-320.453
descent	μ	157.477	-0.103	3770.998	-6.713	0.455	0.02	0.01	0.055	0.486	-0.043	0.057	-80.035
	σ	35.52	0.227	1658.886	3.366	0.171	0.011	0.006	0.033	0.117	0.018	0.558	66.945
	max	228.518	0.35	7088.771	0.019	0.798	0.042	0.021	0.121	0.72	-0.006	1.174	53.856
	min	86.437	-0.556	453.225	-13.446	0.113	-0.002	-0.001	-0.01	0.252	-0.079	-1.06	-213.925
finalapproach	μ	82.325	-0.098	602.514	-4.107	1.246	0.065	0.032	0.022	0.244	-0.051	0.039	-47.038
	σ	14.413	0.231	323.803	1.201	0.403	0.029	0.015	0.009	0.043	0.014	0.182	28.344
	max	111.15	0.365	1250.121	-1.705	2.053	0.123	0.062	0.04	0.33	-0.024	0.403	9.649
	min	53.499	-0.56	-45.092	-6.508	0.44	0.006	0.003	0.004	0.157	-0.078	-0.326	-103.726

Table 6. Result statistics of A380

Phases		V_{TAS}	$\dot{V}_{TAS}$	h	$\frac{dh}{dt}$	C_L	C_D	$C_{D,0}$	K	M	γ	ϕ	$\dot{E}$
take-off	μ	55.367	1.522	0.132	0.201	-	-	-	-	0.163	0.003	-	0
	σ	18.63	0.648	0.982	0.398	-	-	-	-	0.055	0.005	-	0
	max	92.626	2.818	2.097	0.996	-	-	-	-	0.272	0.014	-	0
	min	18.108	0.225	-1.832	-0.594	-	-	-	-	0.053	-0.008	-	0
initialclimb	μ	101.831	0.303	682.336	7.474	1.176	-	-	-	0.302	0.075	0.133	104.869
	σ	20.231	0.453	376.31	3.36	0.409	-	-	-	0.061	0.031	0.837	40.675
	max	142.292	1.209	1434.956	14.194	1.994	-	-	-	0.423	0.137	1.807	186.218
	min	61.37	-0.603	-70.284	0.753	0.358	-	-	-	0.18	0.012	-1.54	23.52
climb	μ	197.955	0.139	4948.045	8.511	0.474	-	-	-	0.62	0.046	0.059	110.803
	σ	32.604	0.247	1971.246	3.506	0.117	-	-	-	0.114	0.024	0.622	51.92
	max	263.163	0.634	8890.538	15.523	0.707	-	-	-	0.847	0.094	1.302	214.642
	min	132.747	-0.355	1005.552	1.499	0.24	-	-	-	0.393	-0.003	-1.185	6.964
cruise	μ	252.015	0.001	11513.164	0.008	0.586	0.021	0.006	0.007	0.853	0.0	0.023	0.394
	σ	23.75	0.274	698.203	0.259	0.153	1.406	0.008	0.011	0.081	0.001	0.462	54.641
	max	299.515	0.549	12909.569	0.526	0.892	2.832	0.021	0.029	1.014	0.002	0.947	109.676
	min	204.514	-0.546	10116.759	-0.51	0.281	-2.791	-0.01	-0.016	0.691	-0.002	-0.902	-108.888
initialdescent	μ	240.494	-0.058	9712.811	-8.076	0.402	0.013	0.007	0.049	0.799	-0.034	0.026	-93.983
	σ	30.549	0.361	1542.392	4.346	0.134	0.008	0.004	0.043	0.108	0.018	0.232	88.464
	max	301.593	0.664	12797.596	0.616	0.67	0.03	0.015	0.135	1.014	0.002	0.491	82.944
	min	179.395	-0.781	6628.027	-16.769	0.135	-0.003	-0.002	-0.036	0.584	-0.07	-0.439	-270.911
descent	μ	155.849	-0.092	3839.285	-6.24	0.468	0.02	0.01	0.053	0.481	-0.04	0.079	-76.089
	σ	35.083	0.198	1675.775	2.978	0.17	0.011	0.006	0.035	0.116	0.017	0.655	47.436
	max	226.016	0.305	7190.836	-0.285	0.807	0.043	0.021	0.123	0.713	-0.006	1.388	18.783
	min	85.682	-0.488	487.735	-12.196	0.128	-0.003	-0.002	-0.016	0.249	-0.074	-1.23	-170.962
finalapproach	μ	82.362	-0.107	592.35	-3.854	1.201	0.06	0.03	0.024	0.244	-0.048	0.041	-47.409
	σ	15.504	0.24	320.112	1.111	0.44	0.03	0.015	0.017	0.047	0.013	0.361	29.181
	max	113.37	0.373	1232.573	-1.632	2.082	0.119	0.06	0.057	0.337	-0.022	0.763	10.954
	min	51.355	-0.586	-47.874	-6.076	0.321	-0.0	-0.0	-0.01	0.151	-0.074	-0.681	-105.772

Table 7. Result statistics of A330-200

Phases		V_{TAS}	$\dot{V}_{TAS}$	h	$\frac{dh}{dt}$	C_L	C_D	$C_{D,0}$	K	M	γ	ϕ	$\dot{E}$
take-off	μ	57.122	1.982	0.0	0.011	-	-	-	-	0.168	0.0	-	0
	σ	17.252	0.753	0.0	0.145	-	-	-	-	0.051	0.002	-	0
	max	91.627	3.488	0.0	0.301	-	-	-	-	0.269	0.004	-	0
	min	22.617	0.475	0.0	-0.279	-	-	-	-	0.066	-0.004	-	0
initialclimb	μ	100.257	0.365	801.686	8.852	1.025	-	-	-	0.297	0.093	0.119	120.611
	σ	20.446	0.784	356.804	4.497	0.376	-	-	-	0.061	0.054	0.567	83.491
	max	141.148	1.933	1515.294	17.845	1.777	-	-	-	0.42	0.2	1.252	287.594
	min	59.365	-1.203	88.078	-0.142	0.273	-	-	-	0.175	-0.014	-1.015	-46.372
climb	μ	188.977	0.134	5247.439	10.087	0.442	-	-	-	0.594	0.057	0.064	121.684
	σ	31.87	0.359	2017.94	4.029	0.119	-	-	-	0.111	0.029	0.685	93.054
	max	252.716	0.852	9283.318	18.145	0.68	-	-	-	0.817	0.115	1.434	307.792
	min	125.238	-0.583	1211.559	2.03	0.204	-	-	-	0.371	-0.002	-1.306	-64.423
cruise	μ	238.868	0.001	11589.581	0.013	0.538	0.038	0.008	0.013	0.808	0.0	0.024	0.201
	σ	23.864	0.185	750.342	0.249	0.155	1.627	0.011	0.102	0.081	0.001	0.594	51.943
	max	286.597	0.371	13090.265	0.511	0.847	3.292	0.03	0.218	0.97	0.002	1.211	104.087
	min	191.139	-0.37	10088.897	-0.486	0.228	-3.215	-0.014	-0.192	0.646	-0.002	-1.164	-103.685
initialdescent	μ	231.815	-0.05	9612.485	-8.546	0.347	0.013	0.006	0.083	0.769	-0.037	0.023	-96.414
	σ	25.628	0.236	1520.818	4.029	0.141	0.008	0.004	0.165	0.091	0.018	0.28	111.46
	max	283.071	0.422	12654.12	-0.489	0.629	0.028	0.014	0.412	0.95	-0.002	0.582	126.505
	min	180.558	-0.522	6570.85	-16.603	0.066	-0.003	-0.001	-0.247	0.588	-0.073	-0.536	-319.334
descent	μ	161.817	-0.093	3856.298	-7.139	0.378	0.017	0.008	0.089	0.5	-0.044	0.045	-85.168
	σ	32.708	0.208	1697.317	3.344	0.17	0.011	0.005	0.152	0.109	0.018	0.327	84.957
	max	227.233	0.323	7250.933	-0.452	0.717	0.038	0.019	0.394	0.718	-0.007	0.7	84.746
	min	96.402	-0.509	461.664	-13.827	0.038	-0.005	-0.002	-0.215	0.281	-0.081	-0.609	-255.083
finalapproach	μ	82.515	-0.12	578.621	-3.935	1.03	0.052	0.026	0.034	0.244	-0.049	0.049	-48.828
	σ	17.332	0.292	315.29	1.348	0.458	0.029	0.015	0.063	0.052	0.015	0.291	42.145
	max	117.179	0.465	1209.2	-1.24	1.945	0.11	0.055	0.16	0.348	-0.019	0.63	35.463
	min	47.852	-0.704	-51.958	-6.631	0.114	-0.007	-0.003	-0.091	0.14	-0.079	-0.533	-133.118

Table 8. Result statistics of B777-200

Phases		V_{TAS}	$\dot{V}_{TAS}$	h	$\frac{dh}{dt}$	C_L	C_D	$C_{D,0}$	K	M	γ	ϕ	$\dot{E}$
take-off	μ	58.554	2.105	0.0	0.002	-	-	-	-	0.172	0.0	-	0
	σ	16.97	1.148	0.0	0.074	-	-	-	-	0.05	0.001	-	0
	max	92.494	4.401	0.0	0.15	-	-	-	-	0.272	0.002	-	0
	min	24.614	-0.191	0.0	-0.146	-	-	-	-	0.072	-0.002	-	0
initialclimb	μ	102.989	0.334	798.953	9.003	0.958	-	-	-	0.306	0.092	0.149	116.511
	σ	18.579	1.465	362.063	3.927	0.299	-	-	-	0.056	0.047	0.82	201.653
	max	140.147	3.264	1523.08	16.856	1.557	-	-	-	0.417	0.185	1.789	519.818
	min	65.83	-2.597	74.826	1.15	0.36	-	-	-	0.194	-0.002	-1.49	-286.795
climb	μ	190.399	0.123	5017.217	10.095	0.444	-	-	-	0.597	0.056	0.064	120.039
	σ	33.037	2.272	2014.548	3.866	0.129	-	-	-	0.115	0.027	0.447	462.866
	max	256.472	4.668	9046.313	17.826	0.702	-	-	-	0.827	0.109	0.958	1045.772
	min	124.325	-4.421	988.12	2.363	0.186	-	-	-	0.367	0.003	-0.83	-805.693
cruise	μ	247.817	0.077	11087.71	0.001	0.484	0.035	0.008	0.014	0.837	0.0	0.034	15.64
	σ	24.975	3.33	759.009	0.201	0.132	1.221	0.009	0.023	0.085	0.001	0.875	766.178
	max	297.767	6.738	12605.729	0.403	0.748	2.477	0.027	0.059	1.006	0.002	1.784	1547.996
	min	197.868	-6.583	9569.691	-0.4	0.221	-2.406	-0.011	-0.032	0.667	-0.002	-1.716	-1516.716
initialdescent	μ	232.444	0.034	9400.682	-8.687	0.322	0.012	0.006	0.068	0.77	-0.038	0.042	-81.099
	σ	26.163	3.345	1432.23	4.719	0.113	0.008	0.004	0.046	0.093	0.02	0.457	881.338
	max	284.769	6.723	12265.142	0.75	0.549	0.027	0.013	0.159	0.955	0.002	0.955	1681.578
	min	180.118	-6.655	6536.223	-18.124	0.096	-0.003	-0.002	-0.024	0.584	-0.077	-0.872	-1843.775
descent	μ	158.625	-0.117	3816.25	-6.838	0.393	0.017	0.008	0.065	0.49	-0.043	0.072	-94.128
	σ	33.629	2.173	1688.249	3.278	0.156	0.01	0.005	0.041	0.112	0.018	0.702	442.078
	max	225.883	4.229	7192.748	-0.281	0.706	0.037	0.018	0.146	0.713	-0.008	1.476	790.028
	min	91.366	-4.462	439.752	-13.394	0.08	-0.003	-0.002	-0.017	0.266	-0.078	-1.333	-978.284
finalapproach	μ	83.334	-0.108	580.164	-4.072	1.013	0.051	0.026	0.028	0.247	-0.05	0.041	-49.88
	σ	15.6	0.93	314.109	1.207	0.39	0.025	0.013	0.015	0.047	0.013	0.278	76.921
	max	114.534	1.752	1208.382	-1.658	1.792	0.101	0.051	0.059	0.34	-0.024	0.596	103.962
	min	52.135	-1.968	-48.054	-6.486	0.233	0.001	0.001	-0.002	0.153	-0.075	-0.514	-203.722

Table 9. Result statistics of B757-200

Phases		V_{TAS}	$\dot{V}_{TAS}$	h	$\frac{dh}{dt}$	C_L	C_D	$C_{D,0}$	K	M	γ	ϕ	$\dot{E}$
take-off	μ	54.149	2.248	0.0	0.006	-	-	-	-	0.159	0.0	-	0
	σ	16.862	1.003	0.0	0.106	-	-	-	-	0.05	0.002	-	0
	max	87.872	4.255	0.0	0.218	-	-	-	-	0.258	0.003	-	0
	min	20.426	0.242	0.0	-0.206	-	-	-	-	0.06	-0.003	-	0
initialclimb	μ	100.91	0.409	870.59	11.199	0.892	-	-	-	0.3	0.116	0.206	152.155
	σ	18.119	0.9	349.209	4.578	0.289	-	-	-	0.054	0.055	0.866	178.192
	max	137.148	2.208	1569.007	20.355	1.469	-	-	-	0.408	0.226	1.938	508.539
	min	64.672	-1.391	172.172	2.043	0.314	-	-	-	0.191	0.005	-1.525	-204.23
climb	μ	191.966	0.182	5173.677	10.987	0.365	-	-	-	0.603	0.061	0.085	147.534
	σ	33.192	0.806	1948.394	4.424	0.097	-	-	-	0.116	0.032	0.774	244.82
	max	258.351	1.794	9070.464	19.835	0.559	-	-	-	0.834	0.124	1.633	637.174
	min	125.582	-1.431	1276.89	2.139	0.17	-	-	-	0.372	-0.003	-1.464	-342.105
cruise	μ	232.757	0.002	11003.885	0.0	0.428	0.03	0.007	0.017	0.785	0.0	0.031	0.5
	σ	24.222	0.415	892.404	0.27	0.106	1.0	0.01	0.039	0.082	0.001	0.722	120.847
	max	281.2	0.831	12788.693	0.541	0.64	2.029	0.028	0.095	0.95	0.002	1.475	242.193
	min	184.313	-0.828	9219.078	-0.541	0.216	-1.97	-0.014	-0.061	0.62	-0.002	-1.414	-241.194
initialdescent	μ	231.841	-0.038	9279.839	-8.974	0.302	0.012	0.006	0.085	0.766	-0.039	0.034	-100.014
	σ	25.592	0.537	1392.58	4.853	0.122	0.008	0.004	0.066	0.088	0.021	0.617	176.166
	max	283.026	1.036	12064.998	0.732	0.547	0.028	0.014	0.217	0.941	0.004	1.267	252.318
	min	180.657	-1.113	6494.68	-18.679	0.057	-0.004	-0.002	-0.047	0.591	-0.082	-1.199	-452.345
descent	μ	164.905	-0.124	3794.116	-8.036	0.35	0.017	0.009	0.09	0.509	-0.049	0.061	-105.402
	σ	35.993	0.558	1662.91	3.9	0.168	0.011	0.005	0.067	0.119	0.02	0.556	214.556
	max	236.891	0.991	7119.935	-0.236	0.685	0.039	0.019	0.224	0.747	-0.009	1.172	323.711
	min	92.919	-1.24	468.297	-15.836	0.015	-0.005	-0.002	-0.045	0.271	-0.089	-1.05	-534.514
finalapproach	μ	79.891	-0.134	607.286	-3.886	1.181	0.062	0.031	0.028	0.237	-0.05	0.06	-51.143
	σ	19.553	0.447	301.335	1.411	0.549	0.034	0.017	0.021	0.058	0.015	0.442	74.582
	max	118.998	0.76	1209.956	-1.063	2.279	0.13	0.065	0.071	0.353	-0.021	0.944	98.022
	min	40.785	-1.028	4.617	-6.709	0.084	-0.006	-0.003	-0.015	0.12	-0.079	-0.823	-200.308

Eurocontrol Aircraft Database

Table 10. Flight performance of A320 obtained from Eurocontrol Aircraft Database[30]

Parameter	Take-off	Initial Climb	Climb	Cruise Climb	Cruise	Initial Descent	Descent	Approach	Landing
$V_{TAS}(m/s)$	75	90	150	220	231	220	145	128	75
$h(m)$	0	1525	4570	8000	12496	8000	3000	1000	0
$\frac{dh}{dt}(m/s)$	0	12	10	5	0	-4	-18	-8	0
M	-	-	-	0.78	0.79	0.78	-	-	-

Table 11. Flight performance of B787-800 obtained from Eurocontrol Aircraft Database[30]

Parameter	Take-off	Initial Climb	Climb	Cruise Climb	Cruise	Initial Descent	Descent	Approach	Landing
$V_{TAS}(m/s)$	85	98	150	224	241	238	154	123	72
$h(m)$	0	1525	4570	8000	13100	8000	3000	1000	0
$\frac{dh}{dt}(m/s)$	0	13.7	10	8	0	-13	-14	-8	0
M	-	-	-	0.79	0.85	0.84	-	-	-

Table 12. Flight performance of A380 obtained from Eurocontrol Aircraft Database[30]

Parameter	Take-off	Initial Climb	Climb	Cruise Climb	Cruise	Initial Descent	Descent	Approach	Landing
$V_{TAS}(m/s)$	77	98	123	260	268	260	154	128	72
$h(m)$	0	1525	4570	8000	13100	8000	3000	1000	0
$\frac{dh}{dt}(m/s)$	0	7.6	12.7	6.6	0	-5	-10	-5	0
M	-	-	-	0.83	0.85	0.83	-	-	-

APE Documentation

The APE tool is the main analysis tool used in this thesis. It tool specially developed functions and classes. In order to extend the usability of the tool outside of this thesis and without the expertise of the author a detailed documentation was made. The full documentation is not appended in the Appendix due to its size. It can be found as an attached document. Now a short overview of the tool can be seen. The APE tool consist of three sub tools. They can be seen as three individual applications, but are bound by the use of the aircraft type object. Each will be discussed in this documentation. The file structure of APE is as follows.

- APE
  - APE tool
    - APE.py: APE is the main analysis script. The user can set analysis parameters such as aircraft type and runtime. By running the script the analysis is initiated.
  - APE viewer
    - viewer.py: The viewer script is used to visualize the results from the APE.py analysis.
  - APE simulator
    - main.py: This script performs the simulation.
    - simlib: Library that houses supporting simulation functions
      - __init__.py
      - editing.py: This module do the waypoint extraction.
      - io.py: This module contains input and output functions. Mainly to communicate with the AircraftType object.
      - plot.py: This module contains functions for plotting.
      - sim.py: This module contains the dynamics and calculation functions.
  - APE lib
    - __init__.py
    - aircrafttype.py: This file contains the AircraftType class, which is used to store aircraft type statistics.
    - flightclass.py: This file contains the Flight class.The Flight objects is where the actual calculation of parameter takes place.
    - aircraftdb.py: This file contains a variable with many aircraft types and corresponding parameters.
    - airportsdb.py: This file contains a variable with many airports and corresponding attributes.
    - aero.py: File containing special functions. See Bluesky documentation for this function.
    - fuzzylog2.py: Module that contains the fuzzy logic used to determine the phase of the measurement.

Acknowledgments

I would like to thank my thesis advisers J. Sun, J. Ellerbroek and J. Hoekstra. Whenever I ran into trouble or had a question about my research or writing it was always easy to reach out. I really value the fact that they allowed this thesis to be my own work. Steering and directions were given, but my opinion appreciated. Finally the pace at which I carried out this thesis would not have been possible without the consent and active collaboration of my advisers.

References

[1]Jacco. M. Hoekstra and Joost Ellerbroek. Bluesky atc simulator project: an open data and open source approach. In *7th International Conference on Research in Air Transportation*, 2016, submitted.

[2]Fligthradar24, 2016.

[3]C Rodney Hanke. The Simulation of a Large Jet Transport Aircraft Volume I: Mathematical Model. *Contractor Report*, pages 1–62, 1971.

[4]Lucio Bianco and Amedeo R Odoni. *Large scale computation and information processing in air traffic control.* Springer, 1993.

[5]Mark E Peters, Mark G Ballin, and John S Sakosky. A multi-operator simulation for investigation of distributed air traffic management concepts. In *AIAA Guidance, Navigation, and Control Conference & Exhibit, Monterey, California, AIAA*, volume 4596, pages 5–8, 2002.

[6]George J Couluris, CG Hunter, Matthew Blake, Karlin Roth, Doug Sweet, Philippe Stassart, James Phillips, and Alex Huang. National airspace system simulation capturing the interactions of air traffic management and flight trajectories. In *AIAA Guidance, Navigation, and Control (GNC) Conference*, 2003.

[7]B.S. Frank Bussink, Ir Jacco Hoekstra, and Ir Bart Heesbeen. Traffic manager: a flexible desktop simulation tool enabling future atm research. In *Digital Avionics Systems Conference, 2005. DASC 2005. The 24th*, volume 1, pages 3–B. IEEE, 2005.

[8]Angela Nuic, Chantal Poinsot, Mihai-George Iagaru, Eduardo Gallo, Francisco A Navarro, Carlos Querejeta, et al. Advanced aircraft performance modeling for atm: enhancements to the bada model. In *24th Digital Avionics System Conference, Washington DC*, 2005.

[9]Yingchuan Zhang, Goutam Satapathy, Vikram Manikonda, and Nikhil Nigam. Ktg: A fast-time kinematic trajectory generator for modeling and simulation of atm automation concepts and nas-wide system level analysis. In *AIAA Modeling and Simulation Technologies Conference*, pages 2–5, 2010.

[10]Damir Poles, Angela Nuic, and Vincent Mouillet. Advanced aircraft performance modeling for atm: Analysis of bada model capabilities. In *Digital Avionics Systems Conference (DASC), 2010 IEEE/AIAA 29th*, pages 1–D. IEEE, 2010.

[11]D Poles. Base of aircraft data (bada) aircraft performance modelling report. *Eurocontrol Experimental Center*, 2009.

[12]European Commission. Report from the commission to the european parliament and the council on the implementation of the single sky legislation: time to deliver., November 2011.

[13]Airbus. A320 dimensions and key data, 2016.

[14]EASA. Icao aircraft engine emissions databank, 2016.

[15]Lorenz Edward. Predictability: Does the flap of a butterfly's wings in brazil set off a tornado in texas? *American Association for the Advancement of Science, Washington, DC*, 1972.

[16]Larry Oolman. Upper air data, 2015.

[17]Daniel Delahaye and Stephane Puechmorel. Tas and wind estimation from radar data. In *Digital Avionics Systems Conference, 2009. DASC'09. IEEE/AIAA 28th*, pages 2–B. IEEE, 2009.

[18]WM Hollister, ER Bradford, and JD Welch. Using aircraft radar tracks to estimate wind aloft. *The Lincoln Laboratory Journal*, 2(3):555–565, 1989.

[19]Junzi Sun, Jacco. M. Hoekstra, and Joost Ellerbroek. Modeling and inferring aircraft takeoff mass from runway ads-b data. In *7th International Conference on Research in Air Transportation*, 2016, submitted.

[20]Junzi Sun, Jacco. M. Hoekstra, and Joost Ellerbroek. Large-scale flight phase identification from ads-b data using machine learning methods. In *7th International Conference on Research in Air Transportation*, 2016, submitted.

[21]de Siebren Haan, de Marijn Haij, and Jan Sondij. The use of a commercial ads-b receiver to derive upper air wind and temperature observations from mode-s ehs information in the netherlands, 2013.

[22]AMP de Leege, MM Van Paassen, and M Mulder. Using automatic dependent surveillance-broadcast for meteorological monitoring. *Journal of Aircraft*, 50(1):249–261, 2012.

[23]AMP De Leege, M Mulder, and MM Van Paassen. Novel method for wind estimation using automatic dependent surveillance-broadcast. *Journal of Guidance, Control, and Dynamics*, 35(2):648–653, 2012.

[24]Richard Alligier, David Gianazza, and Nicolas Durand. Learning the aircraft mass and thrust to improve the ground-based trajectory prediction of climbing flights. *Transportation Research Part C: Emerging Technologies*, 36:45–60, 2013.

[25]Boeing. Boeing website (www.boeing.com), 2016.

[26]Airbus. Airbus website (www.airbus.com), 2016.

[27]Nathan Meier. Jet engine specification database, 2005.

[28]John David Anderson. *Introduction to flight*, volume 199. McGraw-Hill Boston, 2005.

[29]Frederik Michel Dekking. *A Modern Introduction to Probability and Statistics: Understanding why and how.* Springer Science & Business Media, 2005.

[30]Eurocontrol aicraft performance database, 2016.

[31]Dell Adams William Roberson, Robert Root. Fuel conservation strategies: Cruise flight. *Aero Magazine*, 2007.
[32]Bill Roberson. Fuel conservation strategies: Cost index explained. *Aero Magazine*, 2007.
[33]Chris Brady. *The Boeing 737 Technical Guide*. Lulu Press, Inc, 2015.
[34]CFM. Cfm56-3 turbofan engine specifications, 2016.